land

MDPI

Article

Influence of Cumulative Geotechnical Deterioration on Mass Movement at a Medium-Scale Regional Analysis (Cortinas Sector, Toledo, Colombia)

Carlos Andrés Buenahora Ballesteros *, Antonio Miguel Martínez-Graña * and Mariano Yenes

Department of Geology, Faculty of Sciences, University of Salamanca, 37008 Salamanca, Spain; myo@usal.es
* Correspondence: director@ingeotecnia.com.co (C.A.B.B.); amgranna@usal.es (A.M.M.-G.)

Abstract: Landslides in Colombia represent a serious threat to the safety of local communities and the surrounding infrastructure, especially in the mountain range zone. These events occur due to the variation and correlation of endogenous conditions existing in each area, such as geology, geomorphology and coverage, which are triggered by rainfall, seismic events or anthropic activities. This article aims to analyze the geoenvironmental conditions between 2016 and 2021 in the sector known as Cortinas (Toledo, Colombia), applying, for this purpose, the innovative concept of "accumulated geotechnical deterioration" in order to explain the evolution of susceptibility over time from the perspective of prediction, which under traditional methodologies is not properly considered, since unlike what has been thought, the conditioning factors do change in the short and medium term, especially in tropical areas. As a result of this part of the research, the hypothesis was validated that it is necessary for the terrain to be under certain specific conditions for an instability event to occur, which does not depend only on certain critical thresholds of rainfall and earthquakes.

Keywords: landslide; cumulative geotechnical deterioration; susceptibility; hazard zoning

Citation: Buenahora Ballesteros, C.A.; Martínez-Graña, A.M.; Yenes, M. Influence of Cumulative Geotechnical Deterioration on Mass Movement at a Medium-Scale Regional Analysis (Cortinas Sector, Toledo, Colombia). *Land* **2024**, *13*, 1000. https://doi.org/10.3390/land13071000

Academic Editors: Nejc Bezak, Carla Ferreira and Vesna Zupanc

Received: 13 May 2024
Revised: 19 June 2024
Accepted: 1 July 2024
Published: 6 July 2024

1. Introduction

The Colombian national territory exhibits strong geological and geomorphological variation due to the presence of the Andes mountain range. These variations have a substantial geotechnical impact, particularly considering the tropical climatic conditions and frequent seismic activity in the country. As a result, various processes such as mass movement, floods, flash floods, and liquefaction occur [1,2].

Mass movement, as broadly defined by Cruden and Varnes [3], represents an ongoing issue in the Colombian national territory. According to data from the National Unit for Disaster Risk Management, in the last 100 years, 11,800 mass movements have occurred in Colombia [4]. Landslides, whether of soil or rock, involve abrupt movements of the terrain triggered by a combination of factors such as rainfall concentrations, earthquakes, soil/rock properties, slope, and land cover, among others [5,6], or by human activity for development purposes [7,8]. Susceptibility to landslides may be linked to the relationship between geological, geotechnical, geomorphological, hydrological, and ecological conditions, as well as their combinations [9–11]. According to Varnes [12] and Lee and Talib [13], landslides tend to reoccur in areas with existing features or previous movements (morphodynamics). Therefore, it is advisable to consider aspects such as the inventory of movements or deposit areas to establish zones with a higher probability of occurrence [14].

The creation of geotechnical zoning maps assists in identifying areas with a higher probability of landslides occurring. Globally, various methodologies exist, tailored to the criteria and conditions of each region. However, there is no universal regulation governing the development and implementation of geotechnical hazard maps [6,15]. These methodologies vary depending on specific user requirements, intended purpose, scale

of work, data quality, and available resources [6,16]. The using of Geographic Information Systems (GIS) serves as a valuable tool for generating cartographic products, with increasingly widespread application in recent years [17], thereby facilitating the zoning of landslide-prone areas [18,19].

In particular, the UNGRD [20] reported that in the years 2016 and 2021, a total of 332 and 1082 mass movements (respectively) originated in Colombia due to concentrated precipitation seasons and seismic events, affecting nearby infrastructures and communities. However, by the end of 2023 and the beginning of 2024, the phenomenon of El Niño characterized by dry seasons occurred, leading to the formation of certain cracks in the terrain that induced landslides during subsequent rainy periods. This suggests that mass movements are not solely caused by rainfall in a specific season but rather correspond to the combination of different phenomena occurring over time, leading to a gradual deterioration of the soil's resistance capacity until failure occurs.

This article aims to analyze the geoenvironmental conditions between the years 2016 and 2021 in the sector known as Cortinas (Toledo, Colombia), by applying the methodology for hazard assessment at a scale of 1:25,000 developed by the Colombian Geological Survey [21], using the GIS tools of ARGIS 10.8 software and complementing them with the innovative concept of "Cumulative Geotechnical Deterioration" of geological (invariant in the short and medium time), geomorphological (variable) and geotechnical (variable at larger scales) conditioning factors, in order to explain the evolution of susceptibility over time from the perspective of prediction, which under traditional methodologies is not properly considered, which is the problem that leads to this research, since unlike what has been thought, the conditioning factors do change in the short and medium term, especially in tropical areas. The above is highlighted in the conclusions and is expanded upon in Section 5.6.

It is considered pertinent to clarify that the purpose of this research is not to show a new method of hazard assessment that does not rely on the previously mentioned (SGC) to be complemented with the concept of Cumulative Geotechnical Deterioration (CGD). As a second clarification, the SGC methodology is chosen as it is the one currently used in Colombia given its recent publication (2017), but, like others, its effectiveness leaves a high uncertainty [22]. There are other methodologies based on logistic regression, frequency index, decision tree, weight of evidence and artificial neural networks as described by Wang, L. J., Guo, M., Sawada, K., Lin, J., and Zhang, J. [23], which was not considered in the present paper.

The main data correspond to the information collected through engineering works for 33 years of observation that constitute the history of the Cortinas sector and its surroundings, as well as trial and error decisions that have served to feed a deeper investigation from the year 2016, when in the previous year, more than 50 instability events occur in the study area, which affected oil and gas transportation lines, electrical towers, roads and properties. Additionally, we had all the historical information of the instability events presented along the oil and gas transportation lines, a consulting service that we have particularly performed, supplemented by reports, diagnostics, designs and aerial images from different years, as well as the historical memory of professionals and communities that have experienced live the practice of such phenomena. The information of historical records of SIMMA, IDEAM and SGC in relation to old landslides, rains and earthquakes.

2. Study Area

The study area is situated within the jurisdiction of the municipality of Toledo, Norte de Santander, Colombia. It spans approximately 4.5 km in length and has a width of nearly 3 km. The terrain varies in elevation, ranging from approximately 500 to 800 m above sea level (Figure 1).

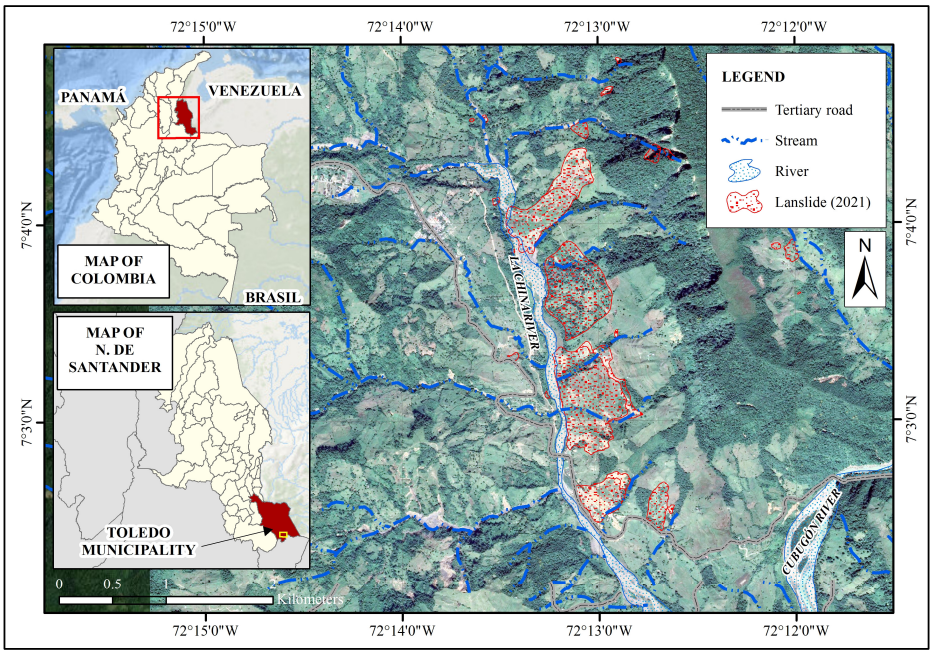

Figure 1. Study area location.

Regional geology positions the study area (Figure 2a) on the north-eastern flank of the Eastern Cordillera of the Andes. This region comprises igneous-metamorphic basement rocks with ages ranging from Precambrian to Paleozoic, underlying sedimentary rocks from the Maracaibo Basin and the Llanero Border sub-basin, which range in age from Mesozoic to Cenozoic, as well as unconsolidated Quaternary sediments. The local geology consists of residual soils and transported deposits (colluvium) of ancient landslides overlying rocks of the San Fernando Formation composed of highly weathered shales susceptible to landslides, with intercalations of harder but highly fractured quartz sandstones.

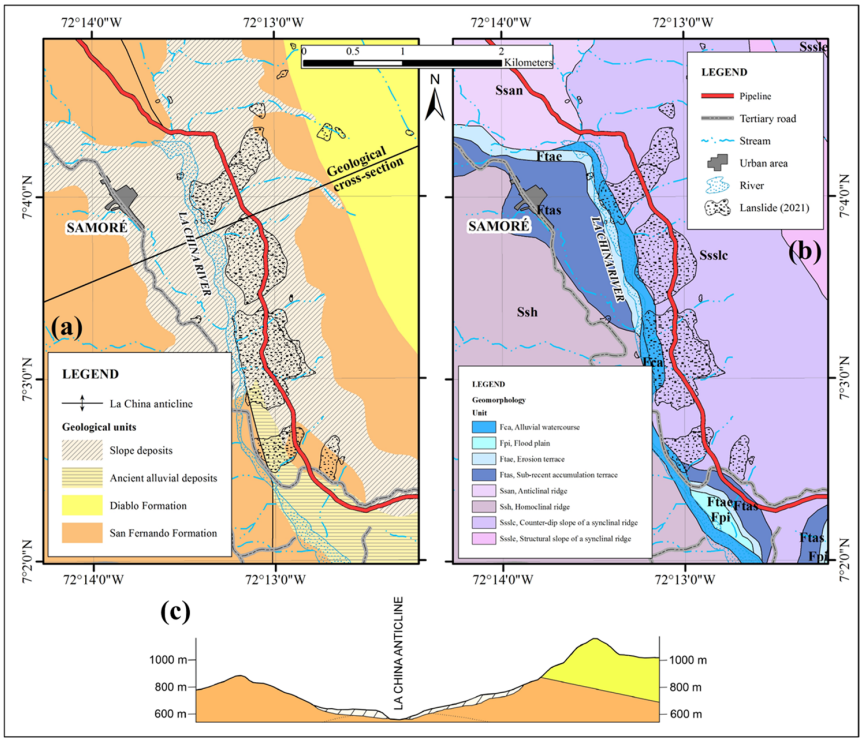

Figure 2. Geological map (**a**), geomorphological map (**b**), and regional geological profile (**c**).

At a tectonic level, an anticlinal structure runs parallel to the La China stream. This structure is likely intersected by geological lineaments in the SW-NE direction, identified through photointerpretation. However, these lineaments are not depicted on the geological map, and further studies or detailed investigations are necessary for their characterization.

The geomorphology (Figure 2b) features steep terrain characterized by prominent escarpments resulting from the lithological properties of the geological formations. Denudation materials generated by weathering, erosion, and transportation via fluvial or gravitational processes are prevalent. Fluvial dynamics from streams like La China and La Tamarana, along with other adjacent streams, contribute to the formation of sedimentation and erosion zones. Additionally, geomorphological units of structural origin, such as the La China anticline associated with folded structures in the area, can be observed (Figure 2c).

3. Background

In particular, the study area known as Cortinas lacks documentary records of geotechnical behavior or initial studies for the construction of existing infrastructure beyond the memory of those who live there. This infrastructure encompasses tertiary and secondary roads, isolated houses, an oil pipeline constructed in 1985 (which experienced a failure in 1990), and a gas pipeline operational since 2011 (Figure 2). In 1990, locals mentioned a mega landslide of the entire hillside, and then in August 2013, a new hillside failure was recorded in the study area, but at specific sites, affecting the gas pipeline, followed by two additional but punctuated failures in 2017.

In 2015, extreme rainfall events led to over 50 landslide sites. These events had a significant impact on the aforementioned infrastructure, resulting in roadblocks and disruptions to the agricultural and livestock activities of the community. Subsequently, assessment, analysis, and mitigation studies of the events were conducted due to the economic losses incurred. However, curiously, the Cortinas slope did not present significant instability events in 2015, a period of extreme rainfall. This situation means that the random causes of the occurrence of these phenomena are studied in a special and different way in order to understand their failure mechanism focused on prediction because, although today the methodologies show some areas of threat, they do not indicate how or when they will occur. The above gives rise to the present research, the beginning of which this document focuses on, without ignoring that to approach a prediction it is required to analyze at larger scales, whose results will be presented in the sequence of future articles at scales 1:5000 and 1:2000, respectively.

The owner of the gas pipeline, aiming to characterize and ensure the integrity of its route, initiated hazard, vulnerability, and risk studies at a 1:100,000 analysis scale, following the methodology provided by the Colombian Geological Survey [24]. Subsequently, methodologies were evaluated at scales of 1:25,000 [21], 1:5000, and 1:2000 [25], which allowed for a more detailed assessment of the general conditions along the pipeline route.

The results of the studies encompassed the Cortinas area, categorizing it as a high-threat zone at the broader scale of 1:100,000 and the semi-detailed scale of 1:5000 (Figure 3). However, detailed stability modeling at a scale of 1:2000 revealed safety factors for maximum earthquake and saturation conditions, indicating a seemingly low threat level and leading to the conclusion that stabilization works were unnecessary. Despite these findings, landslides occurred, resulting in the sudden and catastrophic failure of the gas pipeline. This event generated concern and uncertainty regarding the effectiveness of existing methodologies and the need arose to further investigate the unexpected cause of the landslides and to propose additional concepts in order to clarify the concepts that could not be previously alerted.

According to accounts from the community near the study area, a shallow slope movement occurred in 2020 in the middle zone of the Cortinas sector, covering more than twenty hectares. Confirmation of this event arose once the failure of a nearby gas transmission line was reported. In 2021, three new landslides of approximately one hundred hectares in extension and a volume of mass moved of ten million cubic meters were

triggered. Similar large-scale landslides had already occurred 33 years ago, which are not documented.

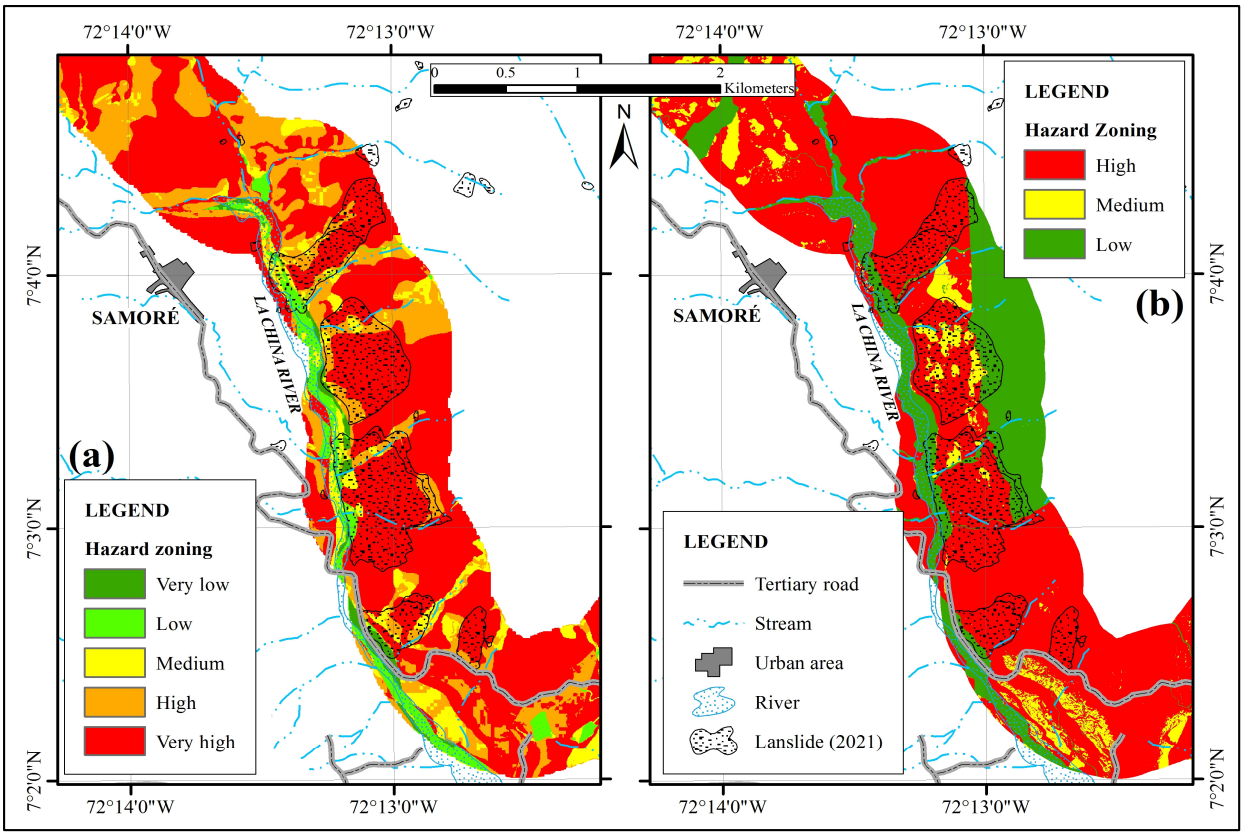

Figure 3. Results of threat studies for the same geographic area: (**a**) 1:100,000 scale, (**b**) 1:5000 scale for images of the year 2017.

The mass movements in the Cortinas sector primarily originated in a wide band of colluvium and residual soils at the top of the slope that washed away the base of very soft and fractured rocks, which became saturated due to the torrential rains on the day of the landslides and in the preceding days. The landslide generated a dragging of material in the direction of the slope including the zones that in the results of the analyses at a detailed scale did not indicate a probable failure, thus deducing that the results of high threat at larger scales should not be discarded but on the contrary should be associated with the results of other smaller scales, as well as involving new concepts to the recently published methods at different scales, since they are presented individually without a proper articulation between them and do not clearly propose the need and the way to update the analyses to consider the deterioration of the terrain in view of its high susceptibility and the constant interaction with the strong triggering factors that occur in the area. The clayey characteristics of both the colluvium and the residual soils contributed to retaining and increasing the water content. But in dry seasons with high temperatures, they have an apparent recovery in their resistance, which makes a behavior prediction model not so easy to define.

The typical failure mechanism in the study area (Cortinas) involves decades of creep processes, followed by rotational and translational failures during extreme rainfall events. Finally, soil and debris flow from previous failures are associated with deforestation and material degradation over the last thirty-three years (Figure 4). Which corresponds to an overlay of an image taken with a drone with 20 cm of resolution, over a satellite image from Google Earth.

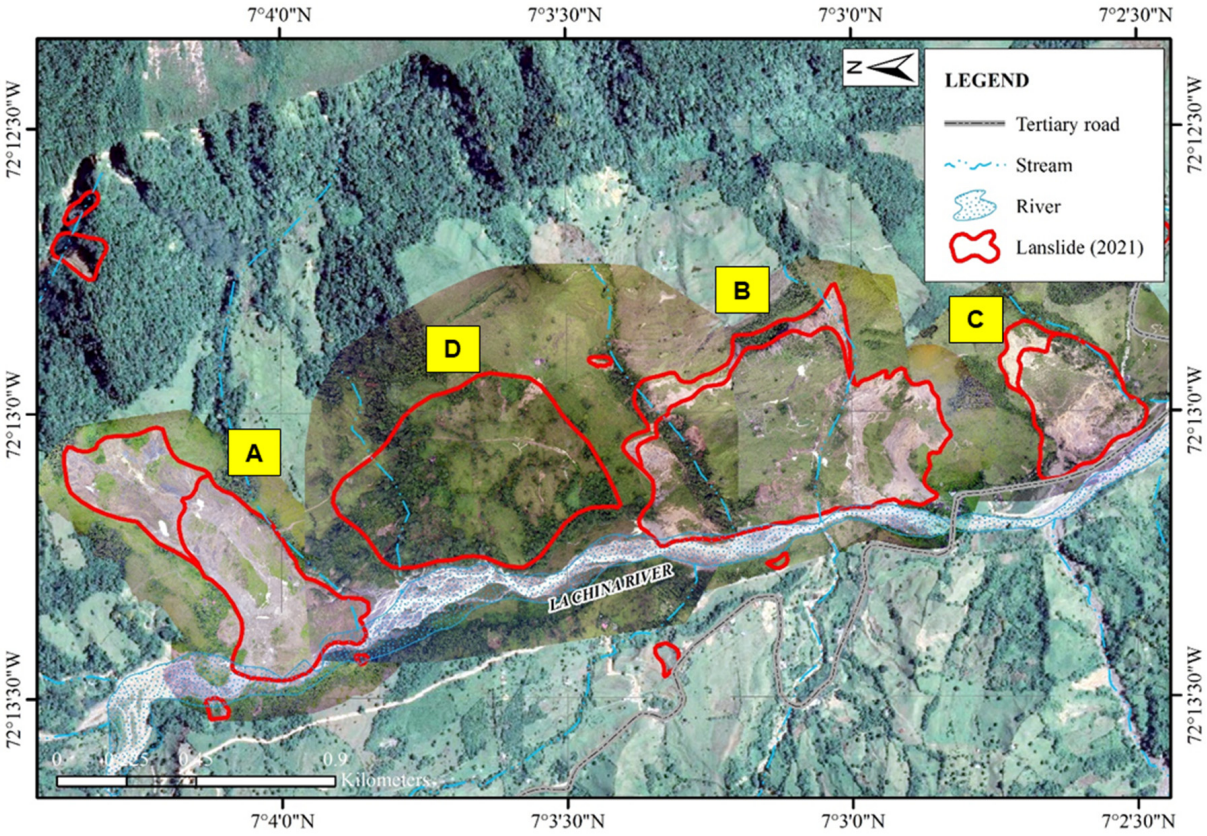

Figure 4. Aerial view of the A, B, C and D landslides developed in the study area.

4. Methods of Analysis

4.1. Hazard Analysis Methodology

This section includes the conceptualization of the methodology used in this study to assess landslide hazard based on the document "Methodological Guide for Landslide Hazard Zoning at a 1:25,000 Scale" provided by the Colombian Geological Service [21], which refers to "Hazard" as the term for dangerousness. This methodology, the results of which are presented below specifically for the Cortinas case, proposes zoning areas susceptible to landslides using Geographic Information Systems (GIS) techniques, gathering and analyzing local-level data on morphodynamic processes, geological and geomorphological characteristics, soil and land cover patterns, as well as hydrological and seismic data. Based on this, the methodology is divided into three main stages for landslide hazard assessment: i. geo-environmental characterization, ii. susceptibility analysis, and iii. hazard analysis.

4.1.1. Geo-Environmental Characterization

In this first stage, the focus is on identifying and analyzing the input variables that determine the occurrence of movements in the terrain considering the following inputs:

Inventory of morphodynamic processes. It visually represents the types of failures, the magnitude of the processes that occur, and their spatial distribution. Additionally, it includes data on erosion and characteristics that suggest possible causes of mass movements. The catalogue and inventory can be developed from primary information sources (residents), secondary information from previous studies, photointerpretation, and field surveys. Subsequently, a cartographic representation of the different types of mass movements is carried out. This study focuses on landslide-type movements [12], as they are the most representative processes in the area.

Conditioning factors. The conditioning factors are a set of spatial data that determine the terrain's propensity to experience mass movements. According to the methodology, these factors should be considered intrinsic or natural to the study area without experiencing

significant changes over time [21]. However, as will be addressed in this study, there is evidence of a degree of deterioration in the natural conditions of the terrain. Thematic maps of geology, geomorphology, and vegetation cover subunits are included as essential inputs in determining mass movements [26], obtained from photointerpretation processes verified in the field. The geological map is represented by surface geological units, which show the surface materials exposed in the terrain, differentiating between soil and rock.

Geomorphology is identified as a potentially dominant factor in the occurrence of new mass movements. It encompasses the history of slope formation, the geometric characteristics that influence its stability, and the genesis of its topography. For landslide hazard zoning in this study, the map of geomorphological units and the slope map are considered. The latter is obtained through analytical processes derived from the Digital Elevation Model (DEM) and classified into ranges from 0° to 90°, as presented in Table 1.

Table 1. Ranges of slope used for engineering analysis and zoning of landslide hazards [21].

Slope	Characteristic Processes and Terrain Conditions
0–2	Flat to nearly flat. No appreciable denudation.
2–4	Gently sloping. Low-speed mass movements and various types of erosion processes, especially under periglacial (solifluction) and fluvial (sheet erosion and rill erosion) conditions. Susceptible to developing erosional processes.
4–8	Sloping. Similar conditions to the previous ones. High susceptibility to developing erosional processes.
8–16	Moderately steep. Mass movements of all types, especially periglacial solifluction, creep, and occasionally slides, as well as laminar and gully erosion. Susceptible to erosion and landslides.
16–35	Steep. Intense denudational processes of different types (erosion under forest cover, creep, landslides). High propensity for the development of erosive process
35–55	Very steep. Rocky outcrops, intense denudational processes, chaotic granular deposits of low thickness.
>55	Extremely steep. Rocky outcrops. Very strong denudational processes, especially "scarp denudation"; susceptible to rock rolling.

Land cover plays a crucial role in landslide behavior. In mountainous areas, especially where natural vegetation has been replaced by agricultural and livestock activities, rapid deterioration of soil properties is observed, increasing vulnerability to landslides. The presence of native trees and natural grasslands in the original ecosystem helps consolidate the soil and improve its ability to maintain hydrogeological stability. The land cover unit map is obtained following the guidelines defined in the Corine Land Cover methodology adapted for Colombia [27].

Triggering Factors. Triggering factors refer to external stimuli on the terrain that modify its stability conditions, such as heavy rainfall or earthquakes [28]. Unlike what Wieczorek [29] (p. 76) mentions—"*Landslides can have several causes, including geological, morphological, physical, and human, but only one trigger*"—mass movements can have different causal factors instead of relying on a single external stimulating factor. It is argued that the combination of different triggers could be the true reason behind the occurrence of the instability phenomenon. Unlike conditioning factors, it is possible to establish frequency and probability parameters based on historical occurrence data within the study area.

According to the methodological guide [21], the calculation of the temporal probability of rainfall-triggered mass movements is addressed in terms of return periods, frequencies, or exceedance probabilities, aiming to characterize each susceptibility category. Statistical analyses are conducted based on rainfall information from the most relevant and nearby hydrological station to the observed movements. The methodology proposes defining the trigger through a simplification of the model. This involves calculating precipitation threshold values prior to the landslide event, exceedance values, and return periods for 24 h of rainfall and cumulative rainfall. However, as noted by Aleotti and Chowdhury [30], a landslide does not always occur when the rainfall threshold is exceeded, as there are other local factors that directly influence it.

On the other hand, the SGC [21] proposes a general approach to the temporal probability of occurrence of an earthquake capable of triggering mass movements. This approach is based on the review of seismicity records available in historical seismic catalogues. Additionally, it involves the application of the theoretical curves presented by Rodríguez, Bommer and Chandler [31].

4.1.2. Susceptibility Analysis

Susceptibility enables the establishment of zones with a higher probability of mass movement occurrence, considering the site's conditioning characteristics [21]. The analysis of susceptibility to mass movements employs the bivariate statistical method of weights of evidence (WofE) [32–36]. It evaluates patterns of association between conditioning factors (evidence) and unstable areas (morphodynamics) by assigning them weights. The weight of each factor is calculated using a Bayesian approach that considers the unconditional and conditional probability of a mass movement occurrence [37].

According to van Westen [38], an effective statistical analysis requires a large number of unstable zones related to various types of mechanisms, along with age information as accurate as possible. Graphically, susceptibility is obtained by the relationship between mass movement and each conditioning factor expressed in terms of pixels for the weights of evidence (W_i), which can be obtained using Equation (1).

$$W_i^+ = \ln \frac{\frac{N_{pix}1}{N_{pix}1+N_{pix}2}}{\frac{N_{pix}3}{N_{pix}3+N_{pix}4}}, \quad W_i^- = \ln \frac{\frac{N_{pix}2}{N_{pix}1+N_{pix}2}}{\frac{N_{pix}4}{N_{pix}3+N_{pix}4}} \tag{1}$$

where the terms Npix are related to the presence or absence of the conditioning factors of mass movement (Table 2).

Table 2. Relationship between landslides and conditioning factor [21].

		Conditioning Factor with Landslide Potential		
		Present	**Absent**	
Landslides	Present	N_{pix1}	N_{pix2}	Total slid area
	Absent	N_{pix3}	N_{pix4}	Total no slid area

The weights of evidence are delineated as outlined in Table 3, where the weight values of the total pixels of each unit of the conditioning factor are categorized based on the occurrence or absence of evaluated landslides, thereby indicating the contribution of that factor to landslides.

Table 3. Weights of evidence definition [21].

Criteria	W_i^+	W_i^-
	Indicates the Importance of the Presence of the Factor in the Landslide	**Indicates the Importance of the Absence of the Factor in the Landslide**
>0	Positive, indicates that the presence of the factor contributes to the occurrence of the landslide; its magnitude indicates the degree of direct correlation or the degree of contribution.	Positive, indicates that the absence of the factor contributes to the occurrence of the landslide.
=0	Indicates that the factor is not relevant.	Indicates that the factor is not relevant.
<0	Negative, indicates that the presence of the factor contributes to the absence of the landslide, with its magnitude indicating the degree of inverse correlation.	Negative, indicates that the absence of the factor contributes to the absence of the landslide.

The total weight contribution for each conditioning factor (W_f) is obtained by summing the negative and positive weights as expressed in Equation (2).

$$W_f = W_i^+ + W_i^- \quad (2)$$

The landslide susceptibility index (LSI) can be obtained by summing the total weights for each conditioning factor in terms of pixels, as expressed in Equation (3).

$$LSI = W_f slope + W_f UGS + W_f geomorphology + W_f LandCover \quad (3)$$

For model calibration, SGC [21] suggests validating it by employing a success curve that indicates percentages for each susceptibility class (high, medium, and low), assuming the failure hypothesis. If the Area Under the Curve (AUC) exceeds 70%, the fit is deemed acceptable. Additionally, utilizing the success curve helps establish the ranges of each susceptibility class based on percentiles and accumulated percentage of landslide pixels.

4.2. Analysis of Hazard and Its Association with Cumulative Geotechnical Deterioration (CGD)

In the methodology (1:25,000), hazard characterization is conducted qualitatively by examining the history of mass movements concerning rainfall and seismic triggers. This process establishes the direct influence and periodicity of events.

In the case of precipitation, this is obtained from the nearest pluviometric station to the study area (Santa María–Abastos station of IDEAM), which allows us to recognize the behavior of rainfall and its influence on the development of landslides. Statistical hydrological calculations were made to determine maximum and minimum values, as well as precipitation thresholds (see Section 5.4). The seismic events on the date of the landslide events, obtained from the national historical seismic record for the zone of influence, are also mentioned.

As outlined in the foundational methodology, identifying morphodynamic processes and compiling a movement inventory are crucial inputs for hazard assessment. However, a significant challenge with this input arises from the scarcity of information including details such as the type of movement, triggering factors, frequency of occurrence, volumes, damages incurred, and even the date of occurrence [39]. These pieces of information are essential for characterizing the movement [40].

According to the above, there are variables associated with time that play a crucial role in determining the occurrence of landslides. Therefore, this study deems it pertinent to introduce the concept of Cumulative Geotechnical Deterioration (CGA) and to consider the geotechnical history of each site. The methodology for hazard assessment by the SGC [21] mentions that "in some cases landslides occur under circumstances where it is not clear what the trigger was, because the variation in different causal factors leads to slopes failing gradually". Guzetti et al. [39] also highlight that, in certain situations, landslides can occur without an evident trigger, or, due to their age, it becomes difficult to link them to a specific factor, thereby establishing a relationship with an intrinsic condition that has been affected over time. This has been named the novel term Cumulative Geotechnical Deterioration (CGD), which is the main objective of this research.

In order to analyze the conditions of CGD in the area, a baseline comparison is proposed between the results of landslide hazard assessment by the SGC for the two years of analysis (2016 and 2021). This comparison enables the quantification of variations that occurred between both periods in the function of each trigger, susceptibility, and hazard, thereby establishing criteria for future research considering the intrinsic and extrinsic conditions of the sector. It is important to clarify that the term CGD is not intended to replace weathering and saprolitization processes, as these processes are associated with rock deterioration over long periods of time. The times of Cumulative Geotechnical Deterioration that occurs in slope deposits of old landslides, which change their strength properties, correspond to shorter periods. This deterioration contributes to the prediction

of when major infrastructure failures may occur in Colombia, a concept that has not been included in the current FRM evaluation models for different scales.

The 1:25,000 scale is approached merely from the geomorphology and vegetation cover, without this representing a limitation but on the contrary the fundamental basis for the determination of the GFD at the geotechnical level at larger scales.

5. Results in the Cortinas Sector

This number includes the analyses conducted for each conditioning and triggering factor in the study area for the two comparison years (2016 and 2021) conceptualized in Section 4.1.

5.1. Inventory of Morphodynamic Processes

Active landslides in the study area were mapped for each analysis year using photogrammetric restitution, represented as polygons (Figure 5).

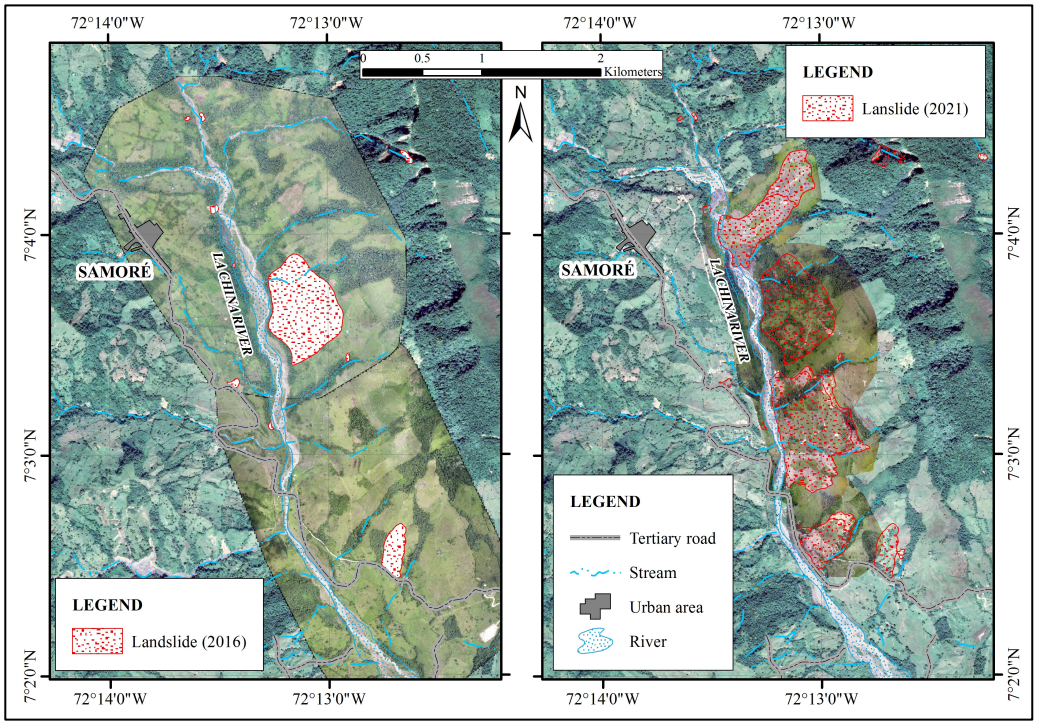

Figure 5. Inventory of morphodynamic processes in the study area: 2016 (**left**) and 2021 (**right**).

5.2. Conditioning Factors

The conditioning factors were derived from aerial photographs captured by an unmanned aerial vehicle with a spatial resolution of 20 cm. This enable geological, geomorphological, and land cover photo-interpretation, which was later validated through direct field inspections.

Geological Factor: In the study area and its surroundings, materials from the San Fernando Formation (Rmmasf) and the Diablo Formation (Rmald) are evident. The San Fernando Formation consists of slates with thin intercalations of fine-grained quartzite sandstone, while the Diablo Formation comprises fine- to medium-grained sandstones interbedded with mudstones. The rock masses of the San Fernando Formation exhibit a moderate degree of weathering (grades III–IV) according to the weathering profile of Dearman [41] and display discontinuity surfaces such as bedding, fractures, and poorly defined joints due to strong folding and fracturing. At the surface level, the massif exhibits a uniaxial compressive strength between 1 and 25 MPa, classifying it as very soft to soft

rock [42]. Discontinuity surfaces (bedding and joints) were recognized in the sandstone layers during field reconnaissance.

The photointerpretation and field inspection work (Figure 6) revealed residual soils from the San Fernando Formation in the area. These soils are characterized as soft, highly plastic, and highly saturated. They are overlain by gravitational transport deposits (colluvial—Stco) which consist of a heterogeneous mixture of sandstone blocks from the Diablo Formation (detached from the upper escarpments) and soil-like materials from the San Fernando Formation. Towards the bottom of the slope, parallel to the course of the Quebrada La China, alluvial deposits (Sta, Stca, Stft) resulting from fluvial dynamics are observed.

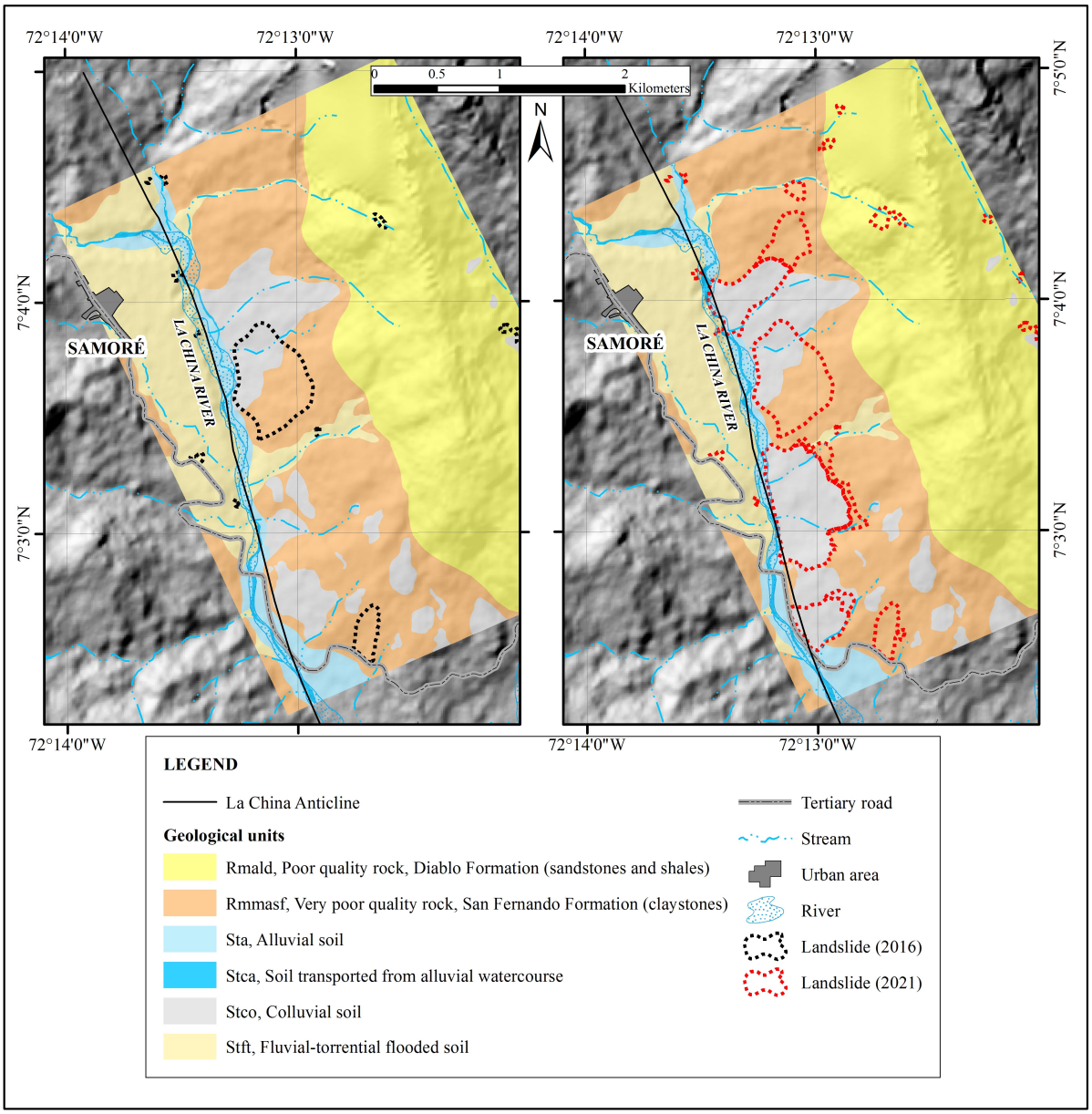

Figure 6. Map of surface geological units in the study area, (**Left**): 2016, (**Right**): 2021.

Geomorphological Factor: The study area exhibits a diverse range of terrain elevations, resulting in significant topographical variability. Prominent geomorphological subunits include erosive slopes (Dle), steep erosive slopes (Dlea), undifferentiated landslide cones (Ddi), colluvial and solifluction lobes (Dco), and debris flow cones or lobes (Dlfd). Fluvial dynamics from the La China and La Tamarana creeks and other adjacent watercourses

create deposition and erosion zones, such as alluvial channels (Fca), floodplains (Fpi), fluvial-torrential fans (Faft), alluvial fans (Fcdy), accumulation terraces (Fta), and fluvial-torrential terraces (Ftft). Structural units associated with the regional structures, such as the synclinal ridge slopes (Sssle) and counter-slope slopes of the synclinal ridge (Ssslc), are observed in the scarps of the Diablo Formation. While landforms of type Dle and Dlea are highly susceptible to various types of landslides with different failure mechanisms, units Ddi, Dco, and Dlfd represent scars and deposits of ancient gravitational processes (Figure 7). Overall, there is no strong variation observed in the geomorphological units in the area; the main changes occur in the areas affected by landslides.

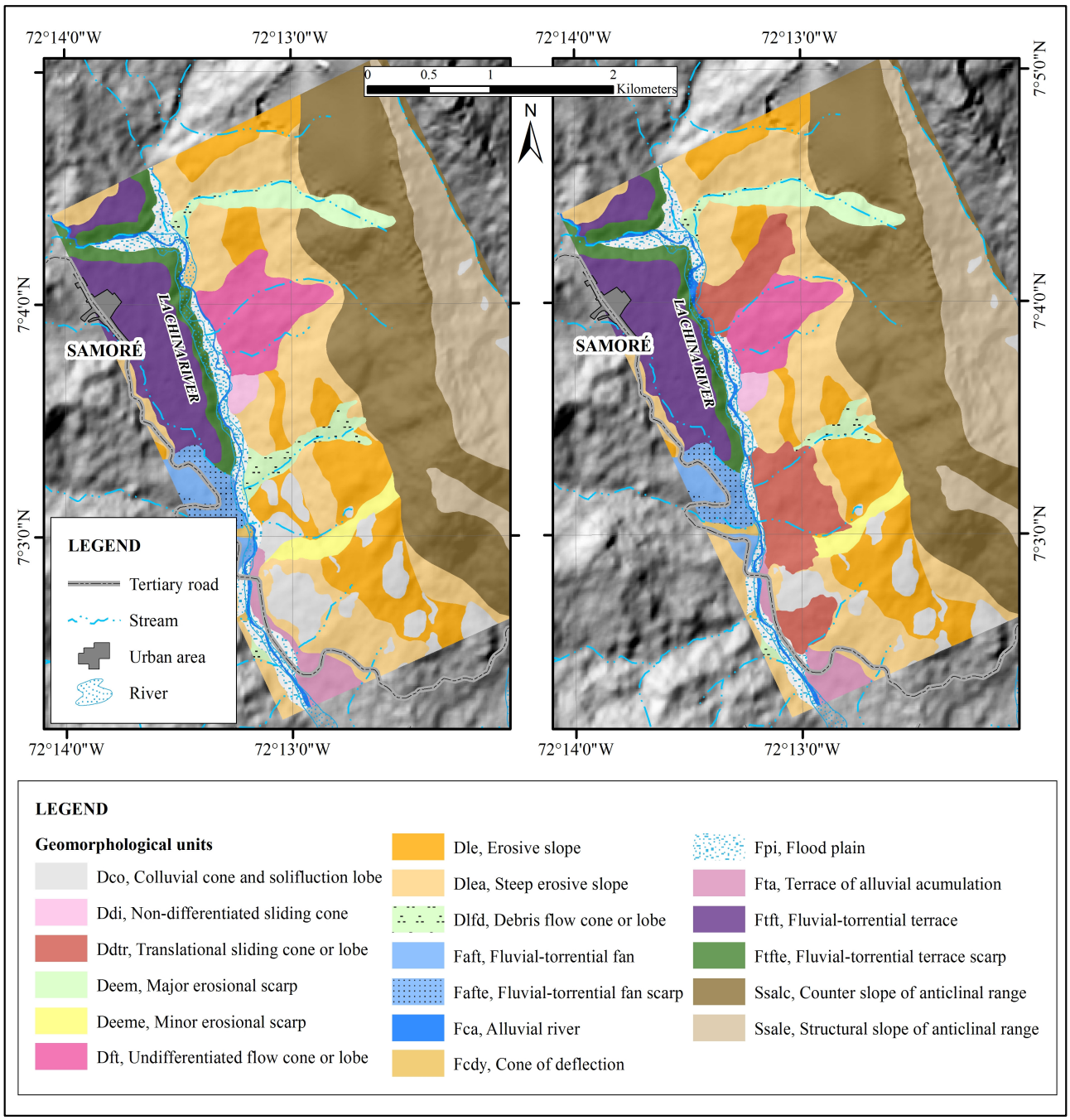

Figure 7. Map of geomorphological units in the study area, (**Left**): 2016, (**Right**): 2021.

Slope factor: The slope was calculated using spatial analysis of the Alos Palsar DEM from the Alaska Satellite Facility, with a spatial resolution of 12.5 m. It was then classified into nine categories, as shown in Table 1. Despite the scale of analysis used for the elevation model, the results of slope classifications are similar between years; however, the weight analysis may be influenced by the presence of landslides each year.

Land Cover factor: The vegetation cover variable was derived from data provided by the Environmental Information System of Colombia (SIAC), which utilizes the Corine Land Cover methodology [27] (Figure 8). In the Troya–Cortinas analysis zone defined by the segmented black line, the light green clean pasture type cover gains area as time progresses, while the Mosaic cover with orange grasses and natural spaces and intermediate green forests decreases in area.

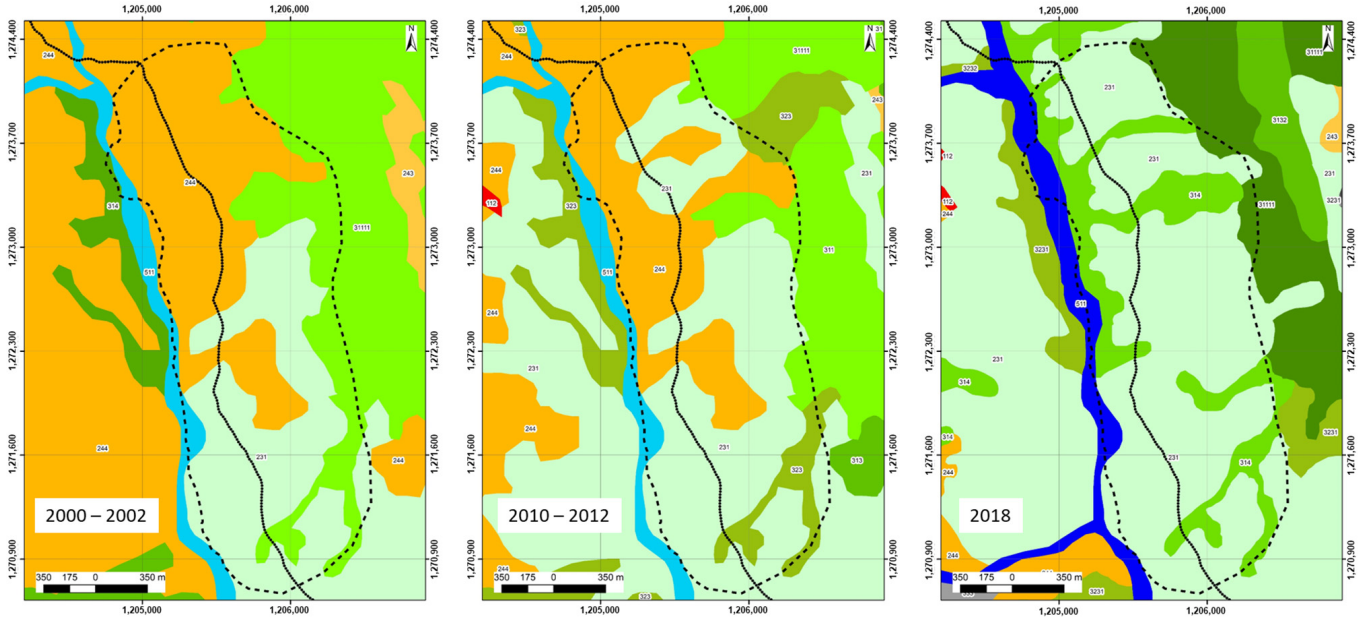

Figure 8. Map of vegetation cover units in the study area, between 2000 and 2018, before the occurrence of the great landslide.

From the previous figure, it is possible to observe the spatial behavior of the cover layers as a conditioning agent for mass movements in the sector between Troya and Cortinas, the site of the emergency. These cover data are presented in time periods between 2000 and 2002, 2010 and 2012 and in 2018, with a periodicity of analysis of 8 years. For this study, the information provided by the SIAC (Environmental Information System of Colombia) was taken from the cover layers elaborated using the Corinne Land Cover methodology, adapted for Colombia by the Institute of Hydrology, Meteorology and Environmental Studies of Colombia (Ideam) (2010).

A detailed analysis of this information reveals the following:

- A constant loss is observed for 18 years, of forest-type coverages and semi-natural areas comprising: dense high terra firme forests, dense forests, dense high terra firme forests and gallery and riparian forests. However, a slight recovery is seen in the 2018 of gallery and riparian forests.
- Secondary, transitional or high vegetation-type coverages have been intermittent during the study periods.
- Heterogeneous agricultural areas comprising pasture mosaics with natural spaces have completely disappeared.
- The areas with mainly clean pastures have been in constant growth and are generally used for economic activities such as cattle raising.

5.3. Susceptibility

The susceptibility was calculated by determining the weight values for each pixel, considering the relationship of the conditioning factors with the occurrence of landslides or unstable areas. Its mathematical development was carried out using Equations (1) and (2) in spreadsheets. GIS tools were utilized to facilitate the obtaining of the required pixel values for the analysis. This process was conducted for each of the conditioning factors, grouping their elements into modeling units (UM) to simplify the study.

The obtained values W_f for each conditioning factor are interpreted as null when the spatial distribution of landslides is not related to the factor under consideration. In the case of a positive association, it indicates that the presence of the factor contributes to the landslide, and the weight will be positive. Conversely, in the presence of a negative association, where the absence of the factor favors the landslide, the weight will be negative (Figure 9).

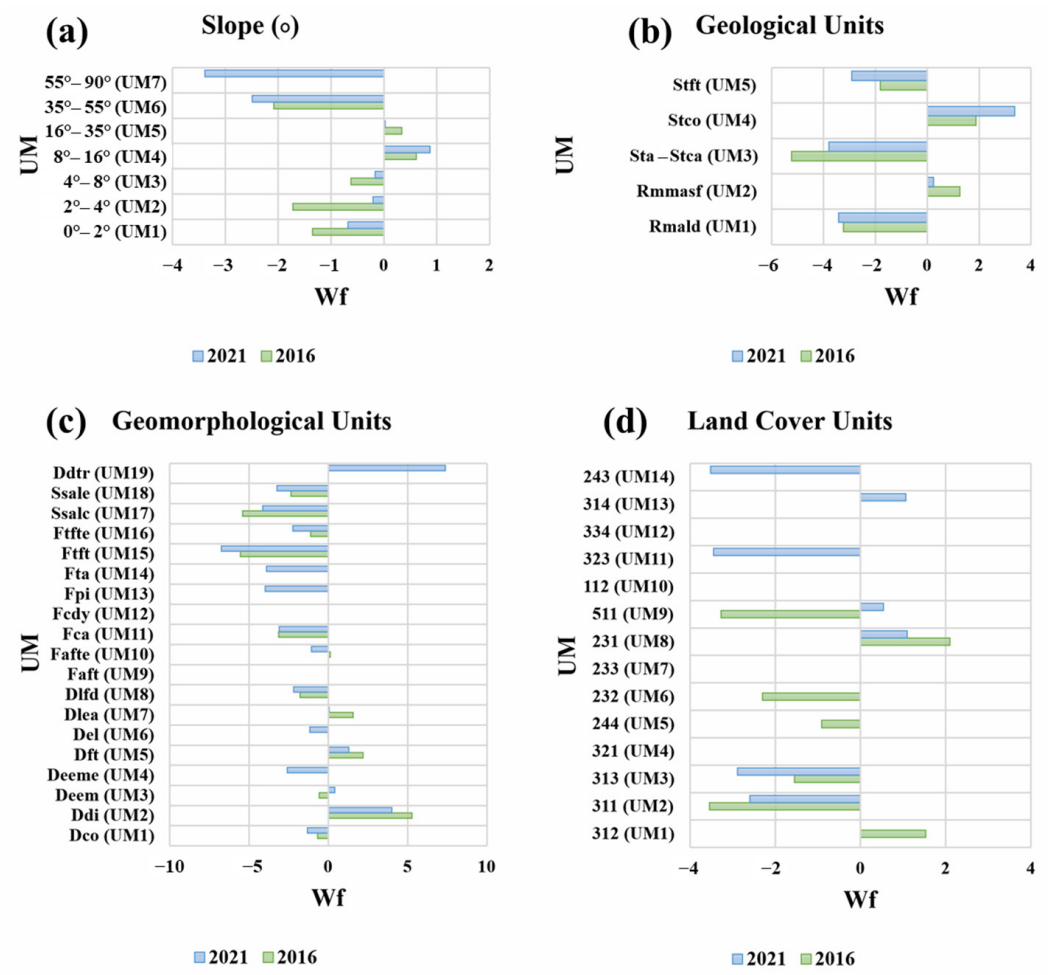

Figure 9. Final weights (Wf) applying the WofE method for the variables slope (**a**), geology (**b**), geomorphology (**c**), and vegetation cover (**d**).

After obtaining the final weights of evidence, it becomes possible to calculate the LSI value for each pixel and then classify them by percentiles. Susceptibility ranges were defined based on success curves for each year, enabling the determination of areas classified as high, medium, and low zoning (Figure 10). Note that the changes in the zoning of the two years of analysis are due to vegetation cover affectation in the two previous decades and modification of the geoform due to landslides in 2021.

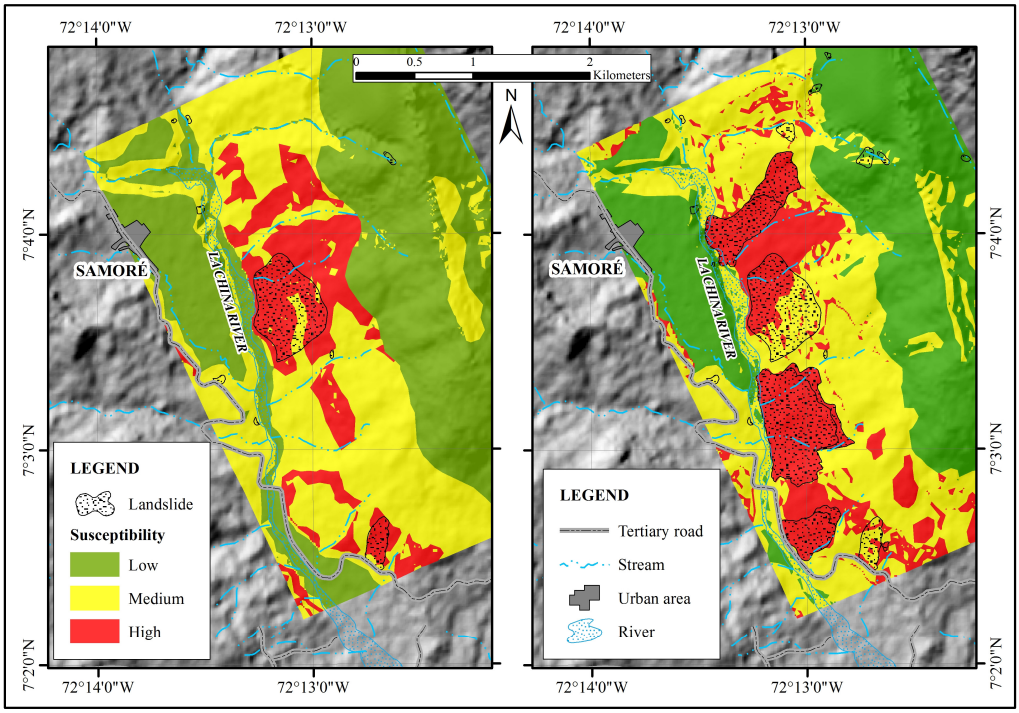

Figure 10. Susceptibility map, (**Left**): 2016, (**Right**): 2021.

5.4. Triggering Factors

Precipitation factor: The SGC [21] has established rainfall thresholds in Colombia based on calculations by Castellanos [43], Moreno et al. [44], Echeverri and Valencia [45], and Ortiz, Penagos and Lizcano [46]. However, these thresholds have not been decisive due to the lack of available information and clear evidence linking rainfall to landslides. Therefore, determining the influence on the threat qualitatively at the 1:25,000 scale is deemed sufficient.

Another crucial consideration is the CGD, as it has been observed that certain rainfall conditions, within the established thresholds, have not triggered landslides at times. This could be because the terrain deterioration has not been sufficient to cause them, despite extreme rainfall values. For landslides to occur, events with multiple variables, which are challenging to determine, must align.

The occurrence of landslides does not solely depend on specific rainfall values, but also on preceding rains, including their intensity, frequency, and duration. Additionally, factors such as soil porosity, hours of sunlight, temperature, and evapotranspiration play significant roles. These variables affecting soil deterioration should be considered in more detailed analyses, where variations in geotechnical parameters and soil mechanical resistance are considered.

For this study, precipitation data were collected from the nearest rain gauge station, the Santa María–Abastos station of IDEAM, covering the period from 1 January 1993 to 31 December 2022. To analyze the rainfall trigger, the number of rainy days per month was considered, ranging from a minimum of 16 days in January to a maximum of 31 days in July. In some cases, rainy days accounted for 80% of the total days of the year.

The graph in Figure 11a shows the mean values for each month. Additionally, the multi-year monthly average precipitation ranged from 349 mm in January and 1078 mm in June, with total annual values generally exceeding 5000 mm (Figure 11b). Moreover, extreme rainfall events, such as the maximum rainfall in 24 h, reached close to 200 mm, particularly in August (Figure 11c).

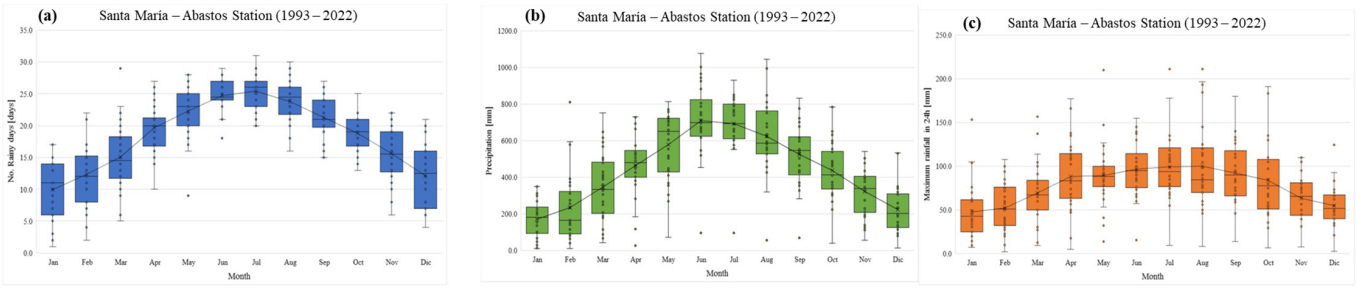

Figure 11. Analysis of rainfall at the Santa María–Abastos rain gauge station. (**a**) Rainy days, (**b**) multiannual mean monthly precipitation and (**c**) maximum monthly 24 h rainfall.

The box and whisker plots provide various statistical data, including minimum, maximum, median, and percentiles.

To determine the causality of the events, the accumulated rainfall in 24 h and in 15 days was determined for landslide records in the Cortinas sector and the surrounding areas influenced by the reported precipitation at the Santa María–Abastos station (Table 4).

Table 4. Landslides and their respective accumulated rainfall.

Data	Cumulative Rainfall Prior to the Landslide		Location
	P 24 h	P15 Days	
3 August 2021	113.0	660.6	Study area
15 January 2020	0.3	78.0	Study area
22 December 2018	0.0	73.5	To 4 km Approx.,
16 February 2018	16.7	123.1	To 6 km Approx.
9 January 2018	27.3	153.6	To 5 km Approx.
20 August 2017	37.2	428.5	Study area
11 August 2017	47.8	497.0	Study area
13 June 2016	12.5	349.4	To 3 km Approx.

With historical data, a threshold is determined to predict the soil's response to rainfall events. However, considering that most landslides occur when there is accumulated rainfall up to the day of the event, thresholds corresponding to the results of antecedent rainfall analysis of 3 days or more have been developed over the years [47]. Figure 12 shows the events presented for the threshold for 24 h of daily rainfall and the antecedent 15 days. The threshold value for the *Y*-axis corresponds to the approximate average value of the maximum daily rainfall over several years, while the *X*-axis corresponds to the average value of the 15 days of antecedent rainfall reported for each landslide event. It is possible to define a trend line that determines the events presented below and above this approximate threshold.

In the previous graph, it can be observed that a consistent threshold is not clearly discernible, as in all cases, 50% of the reported landslide data falls below the proposed threshold [44]. However, the procedure was repeated for rainfall preceding periods of 3, 7, 30, and 90 days prior to the 15 days preceding the landslide date (Figure 13).

Similar behavior is observed to that found for 24 h precipitation, where a clear rainfall threshold cannot be identified due to the wide dispersion of the data. Typically, an attempt is made to define a threshold at which at least 50% of the data points lie above it. This dispersion indicates that landslide events occurred for low values of both daily and accumulated rainfall, undermining the idea that the trigger is exclusively due to a threshold. On the contrary, this supports the notion of accumulated geotechnical deterioration. The occurrence of a landslide is not directly associated with an extreme rainfall event, but rather with the effect of several accumulated rains that generate specific strength conditions leading to failure and develop over time, in combination with other variables. These variables must

be determined as part of another detailed-scale investigation to determine the variation in geotechnical parameters.

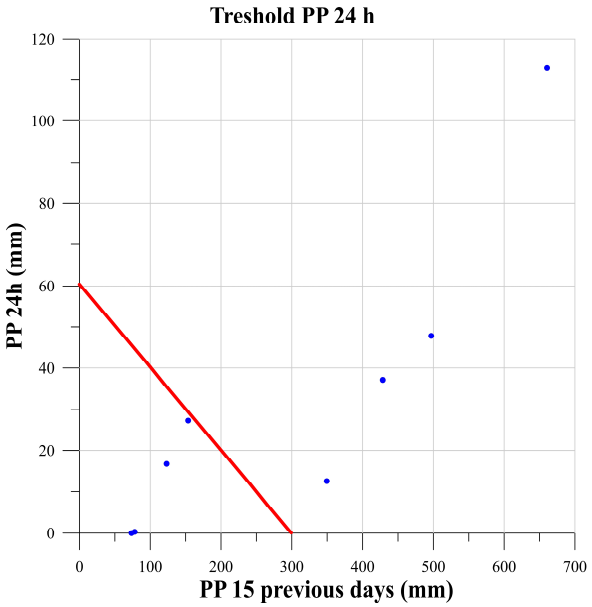

Figure 12. Threshold (red line) for 24 h of preceding rainfall and 15-day antecedent rainfall.

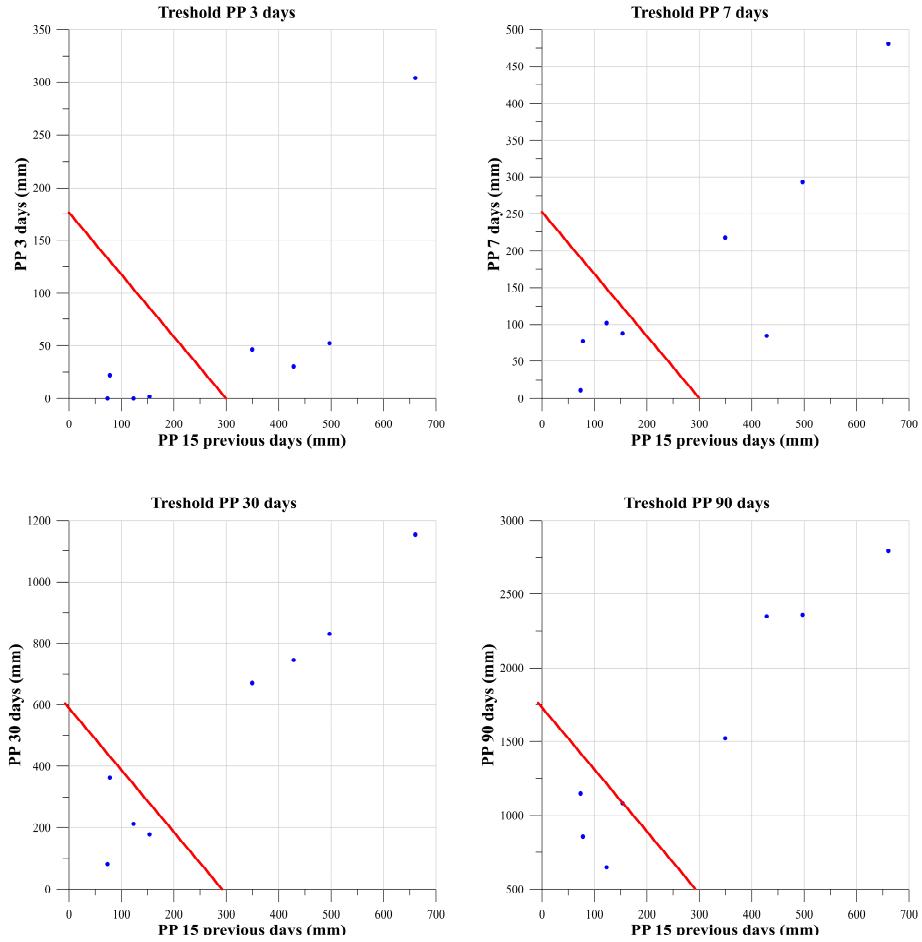

Figure 13. Thresholds (red lines) for various antecedent rainfall configurations, 3 days, 7 days, 30 days, and 90 days.

Seismic Factor: As mentioned in the methodology of the SGC [21], the analysis of earthquakes that trigger landslides is still not sufficiently developed and constitutes a field of research under construction due to the inherent difficulty in defining possible earthquake scenarios, such as the previous moisture conditions and their relationship with the distributions of co-seismic mass movements [48]. Although the peak ground acceleration (PGA) value for this area corresponds to one of the highest in the country, i.e., 0.35 G, the seismic events reported by the SGC in the municipality of Toledo during the years 2016 to 2021 (Appendix A) do not coincide with the dates of the landslides shown in Table 4. However, it could be correlated that whenever an earthquake occurs, there is a contribution to the deterioration of the material which, combined with rainfall events (not necessarily the maximum), contributes to the occurrence of new mass movements.

5.5. Hazard

At the 1:25,000 scale, triggers are considered relevant beyond the criticality of rainfall and seismic threat in the area, which clearly indicates that for a high susceptibility zoning, there is a high threat of landslide occurrence. According to the methodology used, the sector's threat would be mainly influenced by the effects of rainfall alone. In the study area, no seismic events were observed to coincide with the dates of the presented landslides, and it is worth noting that, for Colombia, earthquakes generally occur at great depths (up to 170 km) and with lower magnitudes (most do not exceed a magnitude of 4).

5.6. Cumulative Geotechnical Deterioration of the Sector

The concept of CGD, according to our perception and experience, is proposed as: "It is the degree to which the properties of a soil or rock, which is contemplated within the conditioning factors, tend to decrease or reduce, due to the effect of the triggering factors, constituting a proclivity or facilitating factor for an event related to a mass removal movement to occur at a given moment".

It is called deterioration because it measures the rate, gradient or level of decrease in several of the parameters that determine the resistance of the materials. It is called geotechnical because it refers specifically to soils and rocks that, at a 1:25,000 scale, are limited to geomorphological and vegetation cover change, which are the factors that give rise to geotechnical changes that would be defined in the following articles for 1:5000 and 1:2000 scales. It is said to be accumulated because, through measurement and modeling, the probable magnitudes of the deterioration that should occur are identified and must converge with values of the triggering factors for a landslide event to be activated. It should be noted that in the accumulation of triggering events and in times of drought and long sunny days, there will be a recovery of these properties, and this makes the prediction model complex.

The objective of the measurement and control of the CGD at a scale of 1:25,000 (average) is oriented to determine, by means of anticipated modeling, the set of values that the geomorphological parameters (morphodynamics and morphometry) and vegetation cover may acquire, before the occurrence of a failure or collapse in the terrain, as shown in the flow diagram of (Figure 14) in which, in the case of minimum starting conditions, activities associated with the current practice are developed and, with thicker and dashed lines, three processes are included that are related to the conditioning factors, the modeling of their function and the corresponding control or monitoring.

The minimum starting conditions mentioned above would be as follows:

1. A natural hazard has been identified and characterized.
2. Such hazard has been classified at the high level on the medium 1:25,000 scale.)
3. The methodology for the analysis of mass removal phenomena at a 1:25,000 scale proposed by the Colombian Geological Survey (SGC) in 2017 has been adopted verbatim.
4. It is required to improve the approach to the prediction of ground collapse.

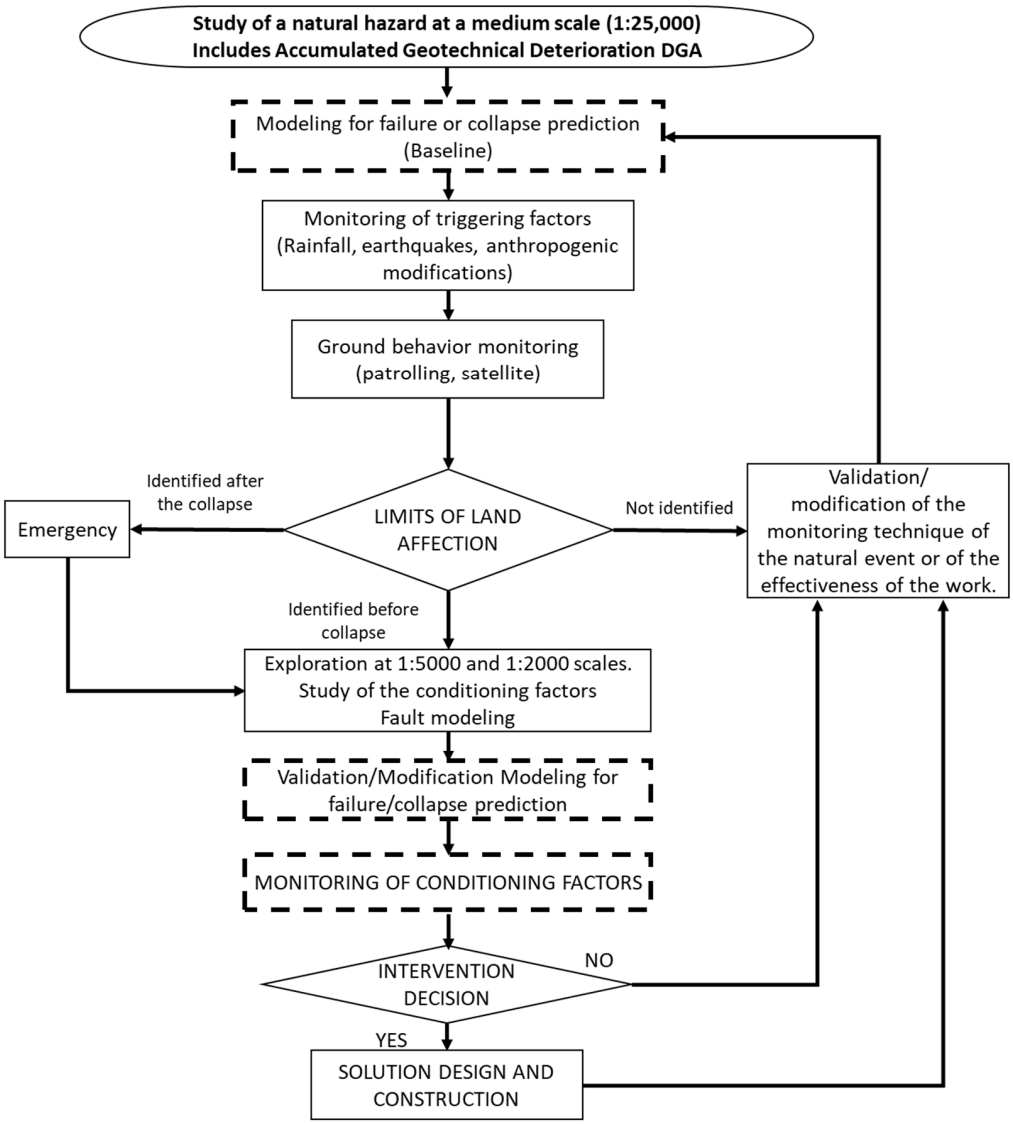

Figure 14. Proposed hazard assessment at a scale of 1:25,000 including the CGD.

The flow diagram of Figure 14 in blocks of continuous line, mentions the processes and decisions that are contemplated in the practice that is carried out today a mass removal phenomenon must be attended. In addition, three blocks with a dashed line border are included, which are three additional components that allow us to differentiate today's practice with the one proposed in this article.

Knowing the starting conditions, the flow chart begins by indicating that a hazard will be studied at a scale of 1:25,000 and that the concept of Cumulative Geotechnical Deterioration will be included; to this end, a process called "modeling for failure prediction" (whose first edition will constitute the "baseline") is started. As indicated, this process is in dashed lines, which means that it is not part of the traditional practice, but it is included because it is part of the novelty proposed in this article. In both cases, both the traditional and the proposed procedure continue with the "monitoring of triggering factors" (rainfall, seismic and anthropogenic), followed by the "monitoring of terrain behavior", which is carried out either by patrolling or by satellite stations or unmanned aircraft.

Finally, a correlation is made between the monitoring of the triggering factors with the "observation of the terrain behavior" in order to determine if the terrain is being affected at a given moment, from which three options for action are established, as follows:

1. If there has not been any ground disturbance yet, there is the option to validate or modify the monitoring techniques being applied; in either case, we return to modeling for failure prediction.
2. If it is identified that the ground has already been affected to the point of collapse, there is definitely an emergency that must be dealt with according to traditional techniques.
3. If it is identified that the ground has indeed been affected, but has not yet collapsed, field explorations are made at a 1:5000 and 1:2000 scale (which will be the subject of future work), and it is determined whether to intervene by means of designs and the corresponding construction. This activity is followed by the validation/modification of the monitoring of the effectiveness of the work. If it is determined not to intervene, the monitoring is continued directly.

As can be seen in the flow diagram. The traditional method, with continuous line blocks, in no case contemplates the CGD, which is based on the variation in the conditioning factors. For this reason, two activities are integrated into this same flow chart before intervening in our proposal:

1. The validation and modification of the modeling for failure prediction.
2. The monitoring of the conditioning factors.

These two activities constitute the other part of the novelty of our proposal.

Unlike most monitoring techniques that are oriented to identify signs of ground failure such as cracking, subsidence, tilting and arching of trees, poles or structures, etc., the control elements on which the CGD focuses are found in the intimacy of the terrain, in its properties. However, the CGD at a scale of 1:25,000 does not consider these parameters and they must be evaluated at detail (5000) and design (2000) scales.

The difference between the CGD and the concepts of consolidation and saprolitization is that the CGD focuses on parameters that are "recoverable", that is, on parameters whose values can oscillate around an average magnitude. Consolidation and saprolitization are phenomena that modify all the properties of the materials; however, once certain magnitudes are acquired, they are not properly "recovered".

According to [21], rainfall thresholds have been established in Colombia according to calculations made by Castellanos [43], Moreno et al. [44], and Echeverri and Valencia [45]. A quantitative comparison of the results obtained between each of the years analyzed is performed in order to establish a baseline that allows evaluation of the accumulated geotechnical deterioration conditions in the study area.

The surface geological units (UGS) show that there was no significant variation in the distribution of geological materials; however, the areas of colluvial deposits increased in both area and distribution due to the landslides that occurred between the years 2016 and 2021 (Figure 7).

The geomorphological variable showed differences in the interpreted units, mainly the morphodynamics represented by mass movements, which exhibited significant variation between one year and another.

The results of the slope did not show significant variation possibly associated with the scale of analysis. It was expected that in the area of landslides, there would be modifications due to the accumulation and detachment of material, as evidenced by some tens of meters high scarps.

The land cover units revealed a significant difference in the areas where landslides occurred, transitioning from grasslands and natural spaces to cleared grasslands, possibly associated with agricultural activities in the region.

It is possible to consider that cover can play a conditioning role in the generation of mass movements, since it can influence the hydrological and mechanical properties of the soil, improving cohesion, strengthening the soil matrix and increasing its matric potential through evapotranspiration and interception. Their intervention can affect soil infiltration and evapotranspiration processes, as well as the capacity of roots to take root in the soil, thus decreasing slope stability and increasing susceptibility to mass movements [49].

Native vegetation covers mainly forests or forest use has a protective effect on rock and soil conditions [49]. As seen in the previous analysis, these forest-type coverages have been disappearing over the years, leaving soils and rocks exposed, negatively influencing the stability of slopes and hillsides. The transition and predominance of pasture-type cover, which is used as grazing areas, has intensified surface erosion processes and has led to a substantial deterioration in the mechanical properties of the soils. Therefore, the cover becomes an important contributor to the generation of mass movements in the area.

There was a significant variation in the high susceptibility zones, which increased from 167.73 Ha to 234.03 Ha. The areas of medium threat showed a slight decrease in the central part of the study area, possibly associated with mitigation works built before the landslide events, which have shown high efficiency. Table 5 shows the area values and percentages of susceptibility classification ranges for the analyzed area in each year.

Table 5. Variation in susceptibility ranges between the years 2016 and 2021.

Susceptibility	2016		2021	
	Area (Ha)	%	Area (Ha)	%
Low	713.57	52.3	604.68	44.3
Medium	482.65	35.4	525.24	38.5
High	167.73	12.3	234.03	17.2

As part of the monitoring conducted since the occurrence of the landslides in August 2021, the following activities have been carried out for one of the landslides (C):

1. Change in vegetation cover by taking aerial images of the landslide 2.
2. Daily rainfall data from 1 March 2023 to 31 May 2024.
3. Topographic monitoring of control points.

For vegetation cover, it was observed that as soon as the landslides occurred in August 2021, much of it was removed by the soil flows; however, by May 2024 a significant recovery was observed, consisting of short grasses except for the escarpments of the movements and an area recently intervened to reestablish the normal transport of the pipeline (Figure 15a,b). In only almost four years, the vegetation was considerably established, which may indicate an apparent and erroneous stable condition for the construction of a new project, and therefore, it is necessary to analyze the geomorphology of the terrain such as changes in slope and morphodynamics to identify the real conditions of stability of the slope. For this, it is vital to have aerial images and topography of different times in order to build the geotechnical history as seen in the sequence of the following images (Figure 15a–c).

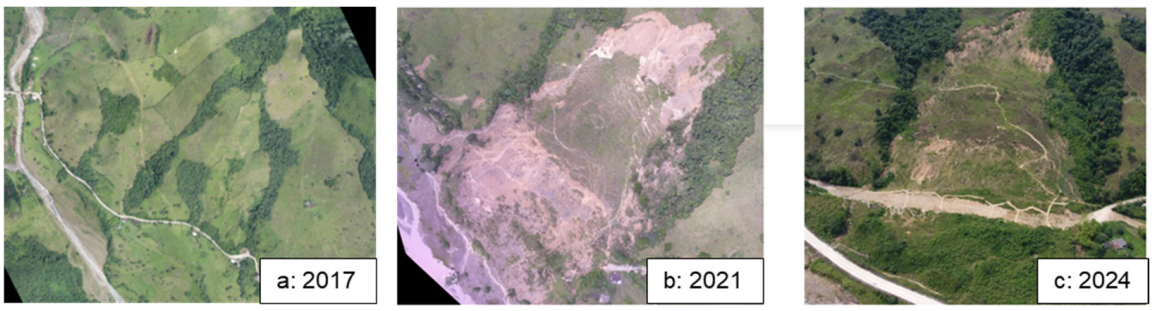

Figure 15. Historical drone imagery 2017 (**a**), 2021 (**b**) and 2024 (**c**) of the study area.

With respect to rainfall data (Table 6), it is observed that in 2015, when about 50 landslides occurred in the study area, rainfall was of significant magnitude but much lower than in 2021 when the Cortinas landslides occurred. On the other hand, in the period analyzed after the Cortinas landslide, there has been rainfall with a similar trend and even slightly higher, and according to topographic monitoring (Figure 16), there have been

no movements beyond a few millimeters. Therefore, it would be expected that for the rains after 2021, large landslides would occur, which has generated uncertainty for the decision-making process to reestablish the service in normal operating conditions of the gas, oil and vehicle transportation lines. It is precisely here where the concept of CGD takes on great relevance since, despite the high rainfall, the terrain is not yet in conditions for large landslides to occur, which indicates that for these to occur, it is not precisely due to thresholds of triggers, but to the resistance of the soil and rocks, part of the CGD that must be analyzed at larger scales of analysis.

Table 6. Cumulative rainfall data for the extreme rainfall periods of 2015, 2021 and 2024.

	Accumulated Precipitation (mm)		
Slope	**26 August 2015**	**3 August 2021**	**30 May 2024**
0–2	74.0	304.2	292.1
2–4	168.0	480.2	437.1
4–8	300.8	660.6	690.6
8–16	643.7	1152.8	1151.3
16–35	1154.5	2087.8	2113.5
35–55	1744.7	2790.5	2803.9

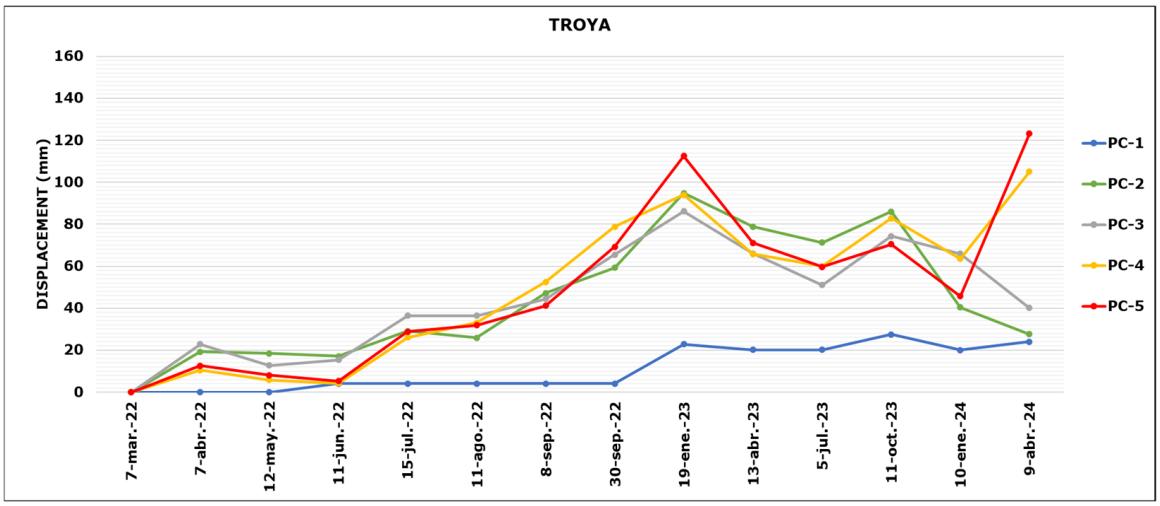

Figure 16. Displacement vs. time monitoring graph.

Regarding the monitoring of landslide, for the instability events of August 2021, ground displacements of approximately 70 m were presented; however, since the subsequent period and to date, it is indicated that the displacements have been small (in the order of mm), contrary to what would be expected, i.e., large displacements for similar or higher rainfall.

To complement the validation of the CGD concept, some cases are listed that failed in the vicinity of the study area with accumulated rainfall well below that of August 2021 when the catastrophic Cortinas landslides occurred. It would be expected that with the magnitude of the 2021 rainfall, the sites listed below would also have failed. Again, the deteriorating ground conditions were not in a position to lead to failure.

5.6.1. Landslide Event in San Bernardo de Bata

On 28 May 2015, near the Gibraltar–Chitagá gas pipeline section, there was a large landslide that swept away some houses (22) and caused a section of the access road to the village of San Bernardo de Bata (300 m) to give way, leaving it out of communication for about four months. It is observed that for the same critical rainfall that triggered a large landslide, the phenomenon would not necessarily be repeated when the precipitation

exceeds this value. It should be noted that the only works carried out after the 2015 landslide were flexible geotextile channels and not retaining works [50].

5.6.2. Landslide Event PK 7 + 860 (Alto de La Muerte)

On 28 August 2013, a landslide was reported that caused the failure of the pipeline at the site known as Alto de la Muerte (Slide B, 2021—Cortinas). This did not fail in the extreme rains of 2015 but failed again and more catastrophically 8 years later in August 2021.

5.6.3. Event PK 9 + 350 (Landslide D intermediate Zone between Landslide A and B Cortinas—2021 (Figure 4)

On 15 January 2020, a rupture of the gas pipeline was reported due to ground failure and as a solution, several rows of micropiles were installed. In August 2021, this site registered deep cracking that doubled the works built in January 2020 but did not fail in a catastrophic and sudden way as it did in the surrounding areas (A and B). However, five years earlier, evaluating the rainiest month reported in the Santa Maria–Abastos station adjacent to the site, we observe that for the date of 15 August 2015, there was accumulated rainfall much higher than the event presented in 2020, but no failure was reported, even without the presence of stabilization works, since by that date, the rows of micropiles had not yet been installed. It is again observed that the same critical rainfall that triggered a ground movement does not necessarily indicate that exceeding this value would generate another landslide. This is explained if the CGD concept is taken into account.

5.6.4. Failure Event PK 23 + 345 (Canoas)

In an area far from Cortinas on 29 June 2022, when one of the months with the highest accumulated rainfall in recent years occurred, there was another similar case where there was breakage of a gas transportation pipeline and strong cracking of the ground; however, this precipitation was exceeded by other events in October 2011 and 2016, there was no failure event. In addition to the above, it is mentioned that in December 2010, a precipitation event of greater magnitude was reported in the sector under study, which caused damage at a point near the Canoas site (PK 26 + 560 to 26 + 190); likewise, despite this event generated failures at another nearby point of the pipeline, in the Canoas sector there were no damages.

6. Discussion

The results of this research show that the influence of drastic changes in vegetation cover can be an important cause of geotechnical deterioration and the consequent occurrence of landslides.

In the same way, it was shown that it is not enough to monitor the triggering factors; it is also necessary to follow up on the changes in the conditioning factors when trying to predict the occurrence of landslide events.

In contrast to what has traditionally been said, changes in the conditioning factors in tropical areas with intense, periodic and long-lasting rainfall regimes and in geologic environments with multiple slope deposits are very common and their measurement is in line with the concept of CGD in landslide prediction. Given that most current hazard zoning methodologies identify areas where instability events may occur, but do not clearly define how and when; although this article reflects the need to involve the concept of CGD to answer these questions, it is opportune to determine how CGD is involved at larger scales (5000 and 1:2000) in relation to the loss of soil resistance to get a little closer to prediction. The use of this concept is not limited only to Colombia; on the contrary, it applies to areas of the world with similar climate and geological conditions. It is considered that it is not appropriate to avoid the respective screening (filter) of the different scales of analysis, since stability should be considered from the macro and micro perspective without losing its correlation and, on the other hand, resorting to "detail" scales to large extensions, would generate long execution times and high costs.

In the case of the 1:25,000 scale (medium), the factors that present changes under the adapted zoning model are vegetation cover, slope changes (morphometry) and new landslide features (morphodynamics). This means that changes at this scale will reflect the decrease in soil resistance parameters, as well as other geotechnical characteristics, which should be taken into account in the analysis of larger scales of detail and design under the same concept of the CGD.

A limitation of the development of this work is that there are no other studies that have involved models where the changes in the conditioning factors (CGD) are included, and therefore, it is recommended to continue documenting and measuring the changes to give greater support from new research by taking aerial or satellite images of high resolution and the implementation of an algorithm based on artificial intelligence that allows systematizing and automating that allows speeding up the monitoring and the consequent early warnings.

Just as the GSC methodology was used for this article to determine the geotechnical hazard zoning at a scale of 1:25,000, the CGD concept is applicable to other methodologies different from the one used here, because it is necessary to implement the monitoring of the conditioning factors when a better approach to the prediction of geotechnical instability events is desired.

However, as mentioned by Aleotti and Chowdhury [30], a landslide does not always occur when the rainfall threshold is exceeded since there are other local factors that have a direct influence, a concept that is part of the considerations of this research to be taken into account in the definition of the CGD.

Given the variety of cases mentioned in this article and events similar to those of Cortinas that are related to the causality of landslides associated with the CGD, no case was found that would indicate a surprising or inconclusive result.

7. Conclusions

The multitemporal analysis of changes in vegetation cover is not the novelty of the research, since this is an input that should be considered as one of the factors describing the accumulated geotechnical deterioration (CGD) for the medium scale (1:25,000) used in the determination of the geotechnical hazard zoning.

The present work showed the results of the application of the landslide hazard methodology for two different years in the sector known as Cortinas (Colombia) and complementary information to date. The two models obtained serve as a basis to establish a comparison factor in the different variables that define the activation of the movements, establishing a new concept defined as accumulated geotechnical deterioration.

Through the application of the methodology indicated by the SGC, specifically focused on the 1:25,000 scale, it was identified among the conditioning factors that it contemplates that, in the short and medium time, vary according to the influence of the triggering factors. Consequently, for this scale, unlike geology, which remains constant in such periods, it became evident that vegetation cover and geomorphology (morphometry and morphodynamics) can be considered as the elements that should be observed in order to establish significant differences in their values over time. Such values influence the behavior and resistance of the soil, a concept we have called Cumulative Geotechnical Deterioration. For triggering factors, it was observed that for the specific case study, there was no relation between the dates of landslides and seismic events. However, it is expected that there is an influence over time contributing to material deterioration, and therefore, it is advisable to conduct additional studies at larger scales such as 1:5000 and 1:2000, which allow quantifying such conditions. As for the rainfall factor, precipitation analyses show a simultaneity between periods of prolonged rainfall and the dates of the presented landslide events, which is a common characteristic in tropical regions, where terrain failure typically occurs due to high levels of precipitation [19,26]. However, a direct association between extreme precipitation values and the occurrence of the event is not observed. Instead, this may be due to the accumulation, frequency, duration, sunlight hours, temperature,

infiltration, changes in pore pressure, and evapotranspiration, among other factors, until failure occurs due to a notable decrease in resistance. This is what we have referred to as Cumulative Geotechnical Deterioration (CGD).

Upon verifying the variation in parameters over the past years based on recent information, consultants' and landowners' recollections, it was found that none of the triggers showed a significant variation over time that alone led to the slope failure. This suggests a convergence with the deterioration of the zone's conditions. Based on this, it can be stated that the state of the conditioning factors in the area influenced the increase in the magnitude of the geotechnical hazard. In other words, over time, geotechnical susceptibility varies depending on the effects of the deterioration of conditioning factors.

A new geotechnical concept is addressed in this study: accumulated geotechnical deterioration (CGD). This refers to the negative change in the intrinsic conditions of terrain characteristics expressed in geological, geomorphological, and vegetative cover terms. The analysis methodology applied to the study area shows that variations in conditioning factors, primarily vegetation cover, influenced the occurrence of landslides observed in the last analyzed year, supported by the increase in areas of high susceptibility. The deteriorated conditions could also be classified as a triggering factor, which should be studied in susceptibility and hazard analyses.

It is considered appropriate to establish baseline trajectories in hazard analyses to recognize the variation in CGD according to the specific conditions of each area, which allows for an approximate projection of possible future events and the development of prior mitigation measures. To achieve this, it is possible to implement periodic monitoring with SAR image analysis and from aerial images, cartographic products, and field surveys. Currently, susceptibility and hazard studies are based solely on current conditions, providing recommendations based on the obtained results without considering the potential advancement of terrain deterioration over time.

The results of this study are related to the scale of analysis (1:25,000); at the specific levels of detail of the 1:5000 and 1:2000 scales, it allows the development, strengthening and deepening of the application of the CGD as an additional component to improve the accuracy in the prediction of a potential landslide event (such scales are part of the following articles associated with this research) to determine with greater precision the mechanism of failure and the direct influence of accumulated geotechnical deterioration on material properties, which could establish some form of deterioration over time.

Author Contributions: Conceptualization, C.A.B.B., A.M.M.-G. and M.Y.; methodology, C.A.B.B., A.M.M.-G. and M.Y.; validation, A.M.M.-G. and M.Y.; formal analysis, C.A.B.B.; investigation, C.A.B.B.; resources, C.A.B.B.; data curation, C.A.B.B.; writing—original draft preparation, C.A.B.B.; writing—review and editing, A.M.M.-G. and M.Y.; visualization, C.A.B.B.; supervision, A.M.M.-G. and M.Y. All authors have read and agreed to the published version of the manuscript.

Funding: This research received no external funding.

Data Availability Statement: The data that support the findings of this study are available upon reasonable request from the authors.

Acknowledgments: The authors thank the company E.D Ingeotecnia S.A.S and especiallyJorge Jiménez, for their technical and strategic support as well as for providing information for the development of this work and Anderson Villamil as support in editing the article. Likewise, to the gas transportation company PROMIORIENTE SA ESP for the constant willingness to allow research to be carried out for the preparation of this article, as well as the following ones on larger scales. This research was assisted by the GEAPAGE research group (Environmental Geomorphology and Geological Heritage) of the University of Salamanca.

Conflicts of Interest: The authors declare no conflicts of interest.

Appendix A

Table A1. Table of seismic records 2016–2021 in the municipality of Toledo, Norte de Santander, Colombia [51].

Date	Latitude	Longitude	Depth (km)	Magnitude (MI)	Date	Latitude	Longitude	Depth (km)	Magnitude (MI)
5 Februrary 2016	7.214	−72.284	0	1.3	8 August 2019	7.248	−72.316	0.25	1.8
8 April 2016	7.179	−72.283	18.8	1.3	24 August 2019	7.265	−72.325	0	2.3
10 June 2016	7.402	−72.166	0	1.9	24 August 2019	7.232	−72.312	0	2.3
5 August 2016	7.28	−72.321	79	1.3	24 August 2019	7.254	−72.323	0	2.6
19 October 2016	7.317	−72.303	122.7	1.6	25 August 2019	7.158	−72.188	3.98	2.2
24 December 2016	7.333	−72.184	28.7	1.4	17 September 2019	7.154	−72.307	0.81	2.3
23 February 2017	7.324	−72.398	87.6	1.4	21 September 2019	7.434	−72.486	0.65	1.4
26 February 2017	7.275	−72.284	68.5	0.9	22 September 2019	7.311	−72.236	0	1.6
8 March 2017	7.317	−72.178	4	2.1	8 November 2019	7.266	−72.174	0	1.6
15 April 2017	7.384	−72.314	8.7	1.1	8 November 2019	7.199	−72.216	0	2.2
29 May 2017	7.389	−72.127	0	1.5	12 November 2019	7.318	−72.184	0	1.8
5 July 2017	7.401	−72.266	4.8	0.8	28 November 2019	7.115	−72.277	0	2.3
31 August 2017	7.305	−72.299	9.5	1.2	12 December 2019	7.097	−72.242	13.07	2.1
21 November 2017	7.36	−72.143	3.9	1.8	14 December 2019	7.099	−72.305	59.3	1.4
25 April 2018	7.113	−72.098	4.8	2.1	3 February 2020	7.075	−72.199	0.12	2.7
19 June 2018	7.078	−72.193	0.23	1.6	8 February 2020	7.104	−72.368	5.41	1.7
14 July 2018	7.147	−72.183	0	2.3	25 February 2020	7.116	−72.366	2.87	1.6
18 July 2018	7.112	−72.165	4	2.4	7 March 2020	7.167	−72.132	−1.7	3
9 September 2018	7.247	−72.41	15.46	1.5	27 May 2020	7.097	−72.153	26.66	1.5
2 October 2018	7.175	−72.319	0.01	1.7	17 June 2020	7.111	−72.202	0	1.9
2 October 2018	7.122	−72.391	29.53	2.2	23 July 2020	7.337	−72.452	0	1.5
2 October 2018	7.224	−72.294	31.17	1.6	23 July 2020	7.39	−72.409	−0.01	1.6
3 October 2018	7.204	−72.385	−0.01	1.6	6 August 2020	6.988	−72.246	1.25	2.2
21 October 2018	7.119	−72.241	3.54	1.8	7 August 2020	7.17	−72.23	21.4	1.5
21 October 2018	7.193	−72.314	0	2.2	12 August 2020	7.388	−72.387	−1.28	2.1
21 October 2018	7.34	−72.271	0	1.7	22 August 2020	7.06	−72.077	0.66	2.3
23 November 2018	7.087	−72.226	4.38	1.3	13 September 2020	7.198	−72.248	0	1.6
2 January 2019	7.148	−72.188	−1.33	1.9	18 September 2020	7.094	−72.345	6.69	1.4
5 January 2019	7.324	−72.47	45.35	1.7	19 October 2020	7.218	−72.17	−1.61	1.7
6 January 2019	7.051	−72.209	1.92	1.5	15 November 2020	7.08	−72.297	16.33	1.8
7 January 2019	7.038	−72.132	0	1.7	7 December 2020	7.012	−72.25	15.86	1.5
17 January 2019	7.092	−72.248	3.7	1.9	2 January 2021	7.047	−72.101	−0.71	2.1
17 January 2019	7.143	−72.168	0.06	2.2	28 January 2021	7.168	−72.131	−1.7	1.9
18 January 2019	7.136	−72.179	3.82	1.8	29 January 2021	7.053	−72.145	14.53	4.3
19 January 2019	7.204	−72.398	−0.02	1.8	2 February 2021	7.101	−72.128	0.94	1.8
23 January 2019	7.128	−72.2	4.1	2.1	13 February 2021	7.139	−72.156	7.08	1.8
23 January 2019	7.117	−72.172	3.29	2.6	30 April 2021	7.147	−72.306	19.14	1.6
24 January 2019	7.129	−72.198	4.94	2	30 April 2021	7.179	−72.273	16.09	1.6
24 January 2019	7.185	−72.189	1.4	1.8	15 May 2021	7.185	−72.31	13.05	1.7
24 January 2019	7.174	−72.166	3.91	2.1	16 May 2021	7.063	−72.284	5.31	1.9
24 January 2019	7.129	−72.193	1.84	2	16 May 2021	7.398	−72.512	13.16	1.6
24 January 2019	7.122	−72.195	2.85	2.3	28 June 2021	7.064	−72.241	1.55	1.8
24 January 2019	7.092	−72.248	4.36	1.9	6 July 2021	7.026	−72.279	10.35	2.2
25 January 2019	7.112	−72.228	4.5	1.6	10 July 2021	7.164	−72.137	0	1.8
11 February 2019	7.05	−72.205	3.84	2	16 July 2021	7.266	−72.198	5.55	1.6
13 February 2019	7.144	−72.24	3.39	1.9	16 July 2021	7.071	−72.096	26.64	2.1
27 March 2019	7.092	−72.125	3.29	1.3	16 July 2021	7.075	−72.1	13.05	1.9
30 March 2019	7.192	−72.352	−0.01	1.4	17 July 2021	7.04	−72.277	26.52	2.4
4 April 2019	7.301	−72.255	15.42	1.7	17 July 2021	7.101	−72.085	2.79	1.8
18 April 2019	7.031	−72.25	3.84	1.6	17 July 2021	7.045	−72.123	23.01	2
6 May 2019	7.094	−72.239	3.73	3.6	17 July 2021	7.07	−72.095	25.35	2.2
8 May 2019	7.296	−72.38	33.17	1.4	8 August 2021	7.118	−72.237	13.05	2
13 May 2019	7.345	−72.2	0	1.7	9 August 2021	7.06	−72.171	0.16	1.7
14 May 2019	7.262	−72.213	0	1.5	25 August 2021	7.058	−72.225	43.55	1.4
18 May 2019	7.204	−72.398	−0.02	1.4	31 August 2021	7.345	−72.264	0	1.6
22 May 2019	7.143	−72.166	4.52	1.9	27 September 2021	7.349	−72.493	21.13	1.9
3 June 2019	7.063	−72.16	7.25	3.2	29 September 2021	7.301	−72.489	0	1.7
3 June 2019	7.076	−72.191	3.57	2.8	8 October 2021	7.071	−72.112	10.75	1.9
4 June 2019	7.073	−72.171	0.34	3.3	25 October 2021	7.207	−72.301	4.61	1.5
19 June 2019	7.328	−72.238	0	1.9	28 October 2021	7.071	−72.169	3.87	1.7
28 June 2019	7.018	−72.248	4.19	1.8	5 November 2021	7.219	−72.25	23.83	1.7
29 June 2019	7.095	−72.264	3.29	1.9	5 December 2021	7.021	−72.251	22.77	2.4

References

1. Körner, C.; Ohsawa, M. 2005. Chapter 24: Mountain systems. In *Ecosystems and Human Well-Being: Current State and Trends*; Hassan, R., Scholes, R., Ash, N., Eds.; Island Press: Washington, DC, USA, 2005; Volume 1, pp. 681–716. Available online: https://www.millenniumassessment.org/en/Condition.html (accessed on 5 March 2024).
2. Slaymaker, O.; Embleton-Hamann, C. Advances in global mountain geomorphology. *Geomorphology* **2018**, *308*, 230–264. [CrossRef]
3. Cruden, D.M.; Varnes, D.J. Landslide Types and Processes. In *Landslides: Investigation and Mitigation, Transportation Research Board*; Turner, A.K., Shuster, R.L., Eds.; Special Report No. 247; Transportation Research Board: Denver, Colorado, USA, 1996; pp. 36–75.
4. Unidad Nacional Para la Gestión del Riesgo de Desastres. n.d. Riesgos por Movimientos en Masa en Colombia. UNGRD. Available online: https://portal.gestiondelriesgo.gov.co/Paginas/Noticias/2020/Riesgo-por-movimientos-en-masa-en-Colombia.aspx#:~:text=De%20acuerdo%20con%20datos%20de,familias%20se%20han%20visto%20afectadas (accessed on 15 December 2023).
5. Anbazhagan, S.; Ramesh, V. Landslide hazard zonation mapping in ghat road section of Kolli hills, India. *J. Mt. Sci.* **2014**, *11*, 1308–1325. [CrossRef]
6. Fayaz, M.; Meraj, G.; Khader, S.A.; Farooq, M.; Kanga, S.; Singh, S.K.; Kumar, P.; Sahu, N. Management of Landslides in a Rural–Urban Transition Zone Using Machine Learning Algorithms—A Case Study of a National Highway (NH-44), India, in the Rugged Himalayan Terrains. *Land* **2022**, *11*, 884. [CrossRef]
7. Skilodimou, H.D.; Bathrellos, G.D.; Kosskeridou, E.; Soukis, K.; Rozos, D. Physical and anthropogenic factors related to landslide activity in the northern Peloponnese, Greece. *Land* **2018**, *7*, 85. [CrossRef]
8. Pacheco, R.; Velastegui-Montoya, A.; Montalván-Burbano, N.; Morante-Carballo, F.; Korup, O.; Deleles, C. Land use and land cover as a conditioning factor in landslide susceptibility: A literature review. *Landslides* **2023**, *20*, 967–982. [CrossRef]
9. Fell, R.; Corominas, J.; Bonnard, C.; Cascini, L.; Leroi, E.; Savage, W.Z. Guidelines for landslide susceptibility, hazard and risk zoning for land use planning. *Eng. Geol.* **2008**, *102*, 85–98. [CrossRef]
10. Bogaard, T.A.; Greco, R. Landslide hydrology: From hydrology to pore pressure. *Wires Water* **2016**, *3*, 439–459. [CrossRef]
11. Valdés Carrera, A.C.; Mendoza, M.E.; Allende, T.C.; Macías, J.L. A review of recent studies on landslide hazard in Latin America. *Phys. Geogr.* **2023**, *44*, 243–286. [CrossRef]
12. Varnes, D.J. *Landslide Hazard Zonation: A Review of Principles and Practice*; Natural Hazard Series; UNESCO: Paris, Italy, 1984; Volume 3, p. 63.
13. Lee, S.; Talib, J.A. Probabilistic landslide susceptibility and factor effect analysis. *Environ. Geol.* **2005**, *47*, 982–990. [CrossRef]
14. Corominas, J.; Moya, J. A review of assessing landslide frequency for hazard zoning purposes. *Eng. Geol.* **2008**, *102*, 193–213. [CrossRef]
15. Da Silva, R.P.; Lacerda, W.A.; Coelho Netto, A.L. Relevant geological-geotechnical parameters to evaluate the terrain susceptibility for shallow landslides: Nova Friburgo, Rio de Janeiro, Brazil. *Bull. Eng. Geol. Environ.* **2022**, *81*, 57. [CrossRef]
16. Manzo, G.; Tofani, V.; Segoni, S.; Battistini, A.; Catani, F. GIS techniques for regional-scale landslide susceptibility assessment: The Sicily (Italy) case study. *Int. J. Geogr. Inf. Sci.* **2013**, *27*, 1433–1452. [CrossRef]
17. Harp, E.L.; Reid, M.E.; McKenna, J.P.; Michael, J.A. Mapping of hazard from rainfall-triggered landslides in developing countries: Examples from Honduras and Micronesia. *Eng. Geol.* **2009**, *104*, 295–311. [CrossRef]
18. Huabin, W.; Gangjun, L.; Weiya, X.; Gonghui, W. GIS-based landslide hazard assessment: An overview. *Prog. Phys. Geogr. Earth Environ.* **2005**, *29*, 548–567. [CrossRef]
19. Do Pinho, T.M.; Augusto Filho, O. Landslide susceptibility mapping using the infinite slope, SHALSTAB, SINMAP, and TRIGRS models in Serra do Mar, Brazil. *J. Mt. Sci.* **2022**, *19*, 1018–1036. [CrossRef]
20. Unidad Nacional Para la Gestión del Riesgo de Desastres. n.d. Consolidado Anual de Emergencias. UNGRD. Available online: http://portal.gestiondelriesgo.gov.co/Paginas/Consolidado-Atencion-de-Emergencias.aspx (accessed on 17 December 2023).
21. Servicio Geológico Colombiano. *Methodological Guide for Hazard Zoning Due to Mass Movements at 1: 25,000 Scale*; Imprenta Nacional de Colombia: Bogotá, Colombia, 2017; (In Spanish). [CrossRef]
22. Wang, L.J.; Guo, M.; Sawada, K.; Lin, J.; Zhang, J. A comparative study of landslide susceptibility maps using logistic regression, frequency ratio, decision tree, weights of evidence and artificial neural network. *Geosci. J.* **2016**, *20*, 117–136. [CrossRef]
23. Reichenbach, P.; Rossi, M.; Malamud, B.D.; Mihir, M.; Guzzetti, F. A review of statistically-based landslide susceptibility models. *Earth Sci. Rev.* **2018**, *180*, 60–91. [CrossRef]
24. Servicio Geológico Colombiano. *Methodological Document for Zoning Susceptibility and Relative Hazard Due to Mass Movements*; Scale 1:100,000; Servicio Geológico Colombiano: Bogotá, Colombiano, 2015. (In Spanish)
25. Servicio Geológico Colombiano. *Methodological Guide for Studies on Hazard, Vulnerability, and Risk Due to Mass Movements*; Imprenta Nacional de Colombia: Bogotá, Colombia, 2016; (In Spanish). [CrossRef]
26. Valencia Ortiz, J.A.; Martínez-Graña, A.M.; Méndez, L.M. Evaluation of Susceptibility by Mass Movements through Stochastic and Statistical Methods for a Region of Bucaramanga, Colombia. *Remote Sens.* **2023**, *15*, 4567. [CrossRef]
27. IDEAM; IGAC; CORMAGDALENA. *Land Cover Map Magdalena-Cauca Basin: CORINE Land Cover Methodology Adapted for Colombia at a Scale of 1:100,000*; Instituto de Hidrología, Meteorología y Estudios Ambientales, Instituto Geográfico Agustín Codazzi y Corporación Autónoma Regional del río Grande de La Magdalena: Bogotá, Colombia, 2008. (In Spanish)
28. Turner, A.K.; Schuster, R.L. *Landslides: Investigation and Mitigation*; National Academy Press: Washington, DC, USA, 1996.

29. Wieczorek, G.F. Landslide triggering mechanisms. In *Landslides Investigation and Mitigation—Special Report N° 247*; Turner, K., Schuster, R., Eds.; Transportation Research Board—National Research Council; National Academy Press: Washington, DC, USA, 1996; Chapter 4; pp. 76–90.
30. Aleotti, P.; Chowdhury, R. Landslide hazard assessment: Summary review and new perspectives. *Bull. Eng. Geol. Environ.* **1999**, *58*, 21–44. [CrossRef]
31. Rodríguez, C.E.; Bommer, J.J.; Chandler, R.J. Earthquake-induced landslides: 1980–1997. *Soil Dyn. Earthq. Eng.* **1999**, *18*, 325–346. [CrossRef]
32. Dahal, R.K.; Hasegawa, S.; Nonomura, A.; Yamanaka, M.; Dhakal, S.; Paudyal, P. Predictive modelling of rainfall-induced landslide hazard in the Lesser Himalaya of Nepal based on weights-of-evidence. *Geomorphology* **2008**, *102*, 496–510. [CrossRef]
33. Regmi, N.R.; Giardino, J.R.; Vitek, J.D. Modeling susceptibility to landslides using the weight of evidence approach: Western Colorado, USA. *Geomorphology* **2010**, *115*, 172–187. [CrossRef]
34. Goetz, J.N.; Brenning, A.; Petschko, H.; Leopold, P. Evaluating machine learning and statistical prediction techniques for landslide susceptibility modeling. *Comput. Geosci.* **2015**, *81*, 1–11. [CrossRef]
35. Lee, J.-H.; Sameen, M.I.; Pradhan, B.; Park, H.-J. Modeling landslide susceptibility in data-scarce environments using optimized data mining and statistical methods. *Geomorphology* **2018**, *303*, 284–298. [CrossRef]
36. Othman, A.A.; Gloaguen, R.; Andreani, L.; Rahnama, M. Improving landslide susceptibility mapping using morphometric features in the Mawat area, Kurdistan Region, NE Iraq: Comparison of different statistical models. *Geomorphology* **2018**, *319*, 147–160. [CrossRef]
37. Bonham-Carter, G.F. *Geographic Information Systems for Geoscientists: Modelling with GIS*; Elsevier: Amsterdam, The Netherlands, 1994; Volume 13. [CrossRef]
38. Van Westen, C.J. *Guidelines for the Generation of 1:50.000 Scale Landslide Inventory, Susceptibility Maps, and Qualitative Risk Maps, Illustrated with Case Studies of the Provinces Thanh Hoa and Nghe An*; University of Twente: Enschede, The Netherlands, 2013. [CrossRef]
39. Guzzetti, F.; Mondini, A.C.; Cardinali, M.; Fiorucci, F.; Santangelo, M.; Chang, K.-T. Landslide inventory maps: New tools for an old problem. *Earth-Sci. Rev.* **2012**, *112*, 42–66. [CrossRef]
40. Van Westen, C.J.; Castellanos, E.; Kuriakose, S.L. Spatial data for landslide susceptibility, hazard, and vulnerability assessment: An overview. *Eng. Geol.* **2008**, *102*, 112–131. [CrossRef]
41. Dearman, W.R. Weathering classification in the characterisation of rock for engineering purposes in British practice. *Bull. Int. Assoc. Eng. Geol.* **1974**, *9*, 33–42. [CrossRef]
42. González de Vallejo, L.I. *Geological Engineering*; Pearson Educación: Madrid, Spain, 2002. (In Spanish)
43. Castellanos, J.R. Critical Rainfall in the Assessment of Mass Removal Event Hazards. Master's Thesis, Universidad Nacional de Colombia, Bogotá, Colombia, 1996. (In Spanish).
44. Moreno, H.A.; Vélez, M.V.; Montoya, J.D.; Rhenals, R.L. Rainfall and Landslides in Antioquia: Analysis of their occurrence on interannual, intrannual, and daily scales. *Rev. EIA* **2006**, *3*, 59–69. (In Spanish). Available online: https://revistas.eia.edu.co/index.php/reveia/article/view/147 (accessed on 12 March 2024).
45. Echeverri, O.; Valencia, Y. Analysis of landslides in the La Iguaná Creek basin in the city of Medellín based on the interaction of rainfall-slope-geological formation. *Dyna* **2004**, *71*, 33–45. (In Spanish). Available online: https://www.redalyc.org/articulo.oa?id=49614204 (accessed on 12 March 2024).
46. Ortiz, D.P.; Penagos, J.C.; Lizcano, A. *Determination of Critical Rains That Trigger Landslides Using Neural Networks*; Uniandes: Bogotá, Colombia, 2002. (In Spanish)
47. Guzzetti, F.; Peruccacci, S.; Rossi, M.; Stark, C.P. Rainfall thresholds for the initiation of landslides in central and southern Europe. *Meteorol. Atmos. Phys.* **2007**, *98*, 239–267. [CrossRef]
48. Corominas, J.; van Westen, C.; Frattini, P.; Cascini, L.; Malet, J.P.; Fotopoulou, S.; Catani, F.; Van Den Eeckhaut, M.; Mavrouli, O.; Agliardi, F.; et al. Recommendations for the quantitative analysis of landslide risk. *Bull. Eng. Geol. Environ.* **2014**, *73*, 209–263. [CrossRef]
49. Pineda, M.C.; Martínez-Casasnovas, J.A.; Viloria, J. Relación entre los cambios de cobertura vegetal y la ocurrencia de deslizamientos de tierra en la serranía del interior, venezuela. *Interciencia* **2016**, *41*, 190–197. (In Spanish). Available online: https://www.redalyc.org/articulo.oa?id=33944256008 (accessed on 16 April 2024).
50. Jacome, J.J. A San Bernardo se lo quiere tragar el agua. *La Opinión J.* **2015**. (In Spanish). Available online: https://www.laopinion.co/region/san-bernardo-se-lo-quiere-tragar-el-agua (accessed on 16 April 2024).
51. Catálogo de sismicidad del Servicio Geológico Colombiano. Available online: http://bdrsnc.sgc.gov.co/paginas1/catalogo/index.php (accessed on 17 December 2023).